# Primary production, new production, and growth rate in the equatorial Pacific: Changes from mesotrophic to oligotrophic regime

Aubert Le Bouteiller, Aude Leynaert, Michael R. Landry, Robert Le Borgne, Jacques Neveux, Martine Rodier, Jean Blanchot, Susan E. Brown

# Primary production, new production, and growth rate in the equatorial Pacific: Changes from mesotrophic to oligotrophic regime

Aubert Le Bouteiller,[1] Aude Leynaert,[2] Michael R. Landry,[3] Robert Le Borgne,[1] Jacques Neveux,[4,5] Martine Rodier,[1] Jean Blanchot,[6] and Susan L. Brown[3]

Received 11 April 2001; revised 5 August 2003; accepted 22 October 2003; published 16 December 2003.

[1] Under an apparent monotony characterized by low phytoplankton biomass and production, the Pacific equatorial system may hide great latitudinal differences in plankton dynamics. On the basis of 13 experiments conducted along the 180° meridian (8°S–8°N) from upwelled to oligotrophic waters, primary production was strongly correlated to chlorophyll a (chl *a*), and the productivity index PI (chl *a*-normalized production rate) varied independently of macronutrient concentrations. Rates of total ($^{14}$C uptake) and new ($^{15}$N-$NO_3$ uptake) primary production were measured in situ at 3°S in nutrient-rich advected waters and at 0° where the upwelling velocity was expected to be maximal. Primary production was slightly higher at the equator, but productivity index profiles were identical. Despite similar $NO_3$ concentrations, new production rates were 2.6 times higher at 0° than at 3°S, in agreement with much higher concentrations of biogenic particulate silica and silicic acid uptake rates ($^{32}$Si method) at the equator. Furthermore, phytoplankton carbon concentrations from flow cytometric and microscopical analyses were used with pigment and production values to assess C:chl *a* ratios and instantaneous growth rates ($\mu$). Growth rates in the water column were significantly higher, and C:chl *a* ratios lower at 0° than at 3°S, which is consistent with the more proximate position of the equatorial station to the source of new iron upwelling into the euphotic zone. For the transect as a whole, compensatory (inverse) changes of C:chl *a* and $\mu$ in response to varying growth conditions appear to maintain a high and relatively invariant PI throughout the equatorial region, from high-nutrient to oligotrophic waters. *INDEX TERMS:* 4231 Oceanography: General: Equatorial oceanography; 4805 Oceanography: Biological and Chemical: Biogeochemical cycles (1615); 4855 Oceanography: Biological and Chemical: Plankton; 4279 Oceanography: General: Upwelling and convergences; *KEYWORDS:* primary production, new production, growth rate, Pacific Ocean, equatorial upwelling, iron

**Citation:** Le Bouteiller, A., A. Leynaert, M. R. Landry, R. Le Borgne, J. Neveux, M. Rodier, J. Blanchot, and S. L. Brown, Primary production, new production, and growth rate in the equatorial Pacific: Changes from mesotrophic to oligotrophic regime, *J. Geophys. Res.*, *108*(C12), 8141, doi:10.1029/2001JC000914, 2003.

## 1. Introduction

[2] The quasi-permanent easterly trade winds blowing across the equatorial Pacific Ocean drive a large-scale zonal circulation whose upwelling divergence brings dissolved carbon and nutrients to the surface. Nutrient-rich waters stretch across 10,000 km of ocean between the Galapagos Islands at 90°W and the 180th meridian, and from 5°N to 5°S. This huge area defined by *Wyrtki* [1981] as the Pacific equatorial upwelling system (''Wyrtki box'') has been estimated to account for 18% of new biological production in the global oceans [*Chavez and Toggweiler*, 1995]. It is also responsible for the greatest efflux of $CO_2$ from the oceans to the atmosphere [*Tans et al.*, 1990], justifying an intensive investigation effort during the International JGOFS Program [*Murray et al.*, 1994].

[3] Extremely low phytoplankton biomass is a well-known characteristic of this broad, persistently nutrient-rich area. *Dupouy et al.* [1993], for instance, calculated a mean surface chlorophyll *a* concentration of 0.203 ± 0.064 mg chl *a* $m^{-3}$ (n = 161 stations) for the Pacific upwelling region. This value is only two times higher than surface chl *a* in severely nutrient-depleted waters in the western tropical Pacific (chl *a* = 0.096 ± 0.062 mg $m^{-3}$; n = 332 stations) [*Dupouy et al.*, 1993] and at station ALOHA in the north subtropical gyre (chl *a* = 0.092 ± 0.007 mg $m^{-3}$) [*Karl et al.*, 1998]. The paradoxical poverty of phytoplankton biomass while macronutrients are permanently above uptake saturation concentrations led *Minas et al.* [1986] to define the high-nutrient, low-chlorophyll (HNLC) concept. The combination of

[1]Institut de Recherche pour le Développement, Nouméa, New Caledonia.
[2]Institut Universitaire Européen de la Mer, Plouzané, France.
[3]Department of Oceanography, University of Hawaii at Manoa, Honolulu, Hawaii, USA.
[4]Observatoire Océanologique de Banyuls (CNRS-UPMC), Laboratoire Arago (UMR 7621), Banyuls sur Mer, France.
[5]Also at Institute de Recherche pour le Développement-Nouméa, Nouméa, New Caledonia.
[6]Institut de Recherche pour le Développement, Sainte-Clotilde, La Réunion, France.


0148-0227/03/2001JC000914

strong micronutrient limitation and grazer regulation of the smallest phytoplankton has been invoked as an explanation for the low chl *a* concentrations during normal (non-El Niño) conditions [*Landry et al.*, 1997]. Despite few concentration measurements, but bolstered by direct evidence from in situ fertilization experiments, iron is well established as the main limiting factor for phytoplankton productivity and biomass [*Martin et al.*, 1991; *Price et al.*, 1994; *Coale et al.*, 1996; *Gordon et al.*, 1997; *Mann and Chisholm*, 2000].

[4] A second characteristic of the equatorial Pacific under normal conditions is the striking spatial monotony of phytoplankton [*Chavez et al.*, 1991; *Le Borgne et al.*, 1999; *Strutton and Chavez*, 2000]. In spite of an intense zonal gradient in nutrients, inversely correlated with sea surface temperature, little geographical variability in chl *a* is evident. During two ALIZE cruises (1965 and 1991) from the Galapagos Islands to the western edge of the equatorial upwelling, surface chl *a* and chl *a* $m^{-2}$ did not differ significantly from one end of the upwelling area to the other [*Le Bouteiller and Blanchot*, 1991]. Even west of the Galapagos, where more than 1 μM of phosphate and up to 10–12 μM of nitrate and silicic acid have been observed [*Guérédrat*, 1971; *Chavez et al.*, 1991; *Reverdin et al.*, 1991; *Chavez et al.*, 1996], surface chl *a* rarely exceeds 0.4 mg $m^{-3}$, as if the same environmental constraints were applied everywhere on phytoplankton biomass. As in a chemostat at steady state [*Frost and Franzen*, 1992], nutrient inputs and all processes increasing the biomass of primary producers must be in a near-perfect balance with all loss processes. Grazing pressure undoubtedly exerts a persistent control on equatorial phytoplankton populations [*Banse*, 1995]. As far as we know, only two exceptions to this monotonously low phytoplankton biomass have been reported to date. The first was a great surface accumulation of buoyant diatoms (*Rhizosolenia*) north of a convergent front in the central Pacific [*Archer et al.*, 1997]. The other was observed on the return to normal conditions after the strong 1997–1998 El Niño episode, when nutrient-rich waters reached the surface and chl *a* increased sharply as in a coastal upwelling [*Chavez et al.*, 1999].

[5] A third typical feature of the equatorial Pacific HNLC system is the phytoplankton size structure. During the ALIZE 2 cruise, chl *a* was almost equally distributed into 3 main size classes,<1 μm, 1–3 μm and >3 μm (39, 33 and 28% respectively, means of 42 profiles) which remained nearly constant along the equatorial belt from 95°W to 167°E [*Le Bouteiller and Blanchot*, 1991]. Hence, the <3 μm size fraction clearly and systematically dominates the phytoplankton, even in upwelled waters [*Chavez*, 1989; *Peña et al.*, 1990; *Le Bouteiller et al.*, 1992]. This small size class is composed of *Prochlorococcus*, *Synechococcus* and picoeukaryotic algae [*Blanchot et al.*, 2001; *Mackey et al.*, 2002a] which have greater surface area:volume ratios and should be less diffusion limited by trace metals than larger cells [*Morel et al.*, 1991; *Thingstad*, 1998]. Conversely, small cells support a stronger grazing pressure than larger cells [*Legendre and Le Fèvre*, 1989] because grazing is mainly due to protozoans with division rates similar to or higher than those of phytoplankton, allowing rapid responses in grazing pressure to any change of food supply [*Banse*, 1994].

[6] Because of intense protistan grazing on small cells, ammonium is excreted, either directly or via mesozooplankton [*Raimbault et al.*, 1999; *Gaudy et al.*, 2003]. Since ammonium is the preferred nitrogen source for uptake by phytoplankton [*Dortch*, 1990; *Wheeler and Kokkinakis*, 1990], a fourth characteristic of the equatorial Pacific is the large and systematic predominance of regenerated production over new production [*Dugdale and Wilkerson*, 1991; *Dugdale et al.*, 1992; *McCarthy et al.*, 1996; *Raimbault et al.*, 1999, 2000]. As suggested by *Walsh* [1976], the low frequency of variability of the physico-chemical habitat of the equatorial divergence promotes the evolution of herbivorous populations, which markedly influence and control phytoplankton size, species composition and nutrient utilization.

[7] Since the main properties of phytoplankton exhibit a narrow range of variability and a quasi-uniform distribution within the Wyrtki box, the major processes controlling fluxes of energy and matter should be persistent (but not necessarily constant) in the system, which would facilitate their description and modeling. In the present paper, we report data from experiments intended to analyse the relationship between particulate organic carbon production and phytoplankton biomass, and to determine if and how chlorophyll *a* can be used to predict primary production in the western equatorial Pacific. For that purpose, plankton populations were sampled from 8°S to 8°N along the trophic gradient from extreme oligotrophy to the north and south and typical HNLC conditions in the equatorial upwelling zone.

[8] In addition, to better understand the processes involved in the upwelling system, phytoplankton dynamics were studied in detail at two stations located at 3°S and on the equator and occupied during 5 days of intensive sampling. The aim was to investigate the potential biological consequences of two slightly different chemical and hydrological structures. In a previous paper, a clear change of silicic acid limitation of diatom silica production was evident between the two time series stations [*Leynaert et al.*, 2001]. Here, we complete the analysis by comparing results of in situ measurements of primary production, new production ($NO_3$ uptake) and silicic acid uptake. Our observations show that equatorial waters are more productive in terms of nitrate and silica uptake at 0° than at 3°S. Thus, in spite of only slight variations of phytoplankton biomass, size structure, cell composition and primary production, strong differences of new production fluxes may occur at different locations within the HNLC region.

## 2. Material and Methods

### 2.1. Sampling, Nutrients, Pigments, Flow Cytometry, and Phytoplankton Carbon

[9] The Etude du Broutage En zoNe Equatoriale (EBENE)-JGOFS cruise of R/V *L'Atalante* (21 October to 20 November 1996) consisted of transect sampling along the dateline, with stations occupied every degree of latitude from 8°S to 8°N and two time series stations at 3°S and the equator. Water column properties were sampled routinely to 300 m by CTD rosette, with discrete samples at 12 depths. Temperature, salinity, currents and nutrients (nitrate, nitrite, ammonium, phosphate and silicic acid) measurements are described in detail by *Eldin and Rodier* [2003].

[10] In all samples collected for production measurements, chlorophyll pigments were analysed by both spectrofluorometric and fluorometric techniques. For discrimination of monovinyl- and divinyl-chlorophyll *a* by spectrofluorom-

**Table 1.** On-Deck Experiments[a]

| Latitude | Date | Temperature | $NO_3$ | $NO_2$ | $PO_4$ | $Si(OH)_4$ | Syn. | Proc. | Pico. | |
|---|---|---|---|---|---|---|---|---|---|---|
| 8°02S | 10–26 | 29.312 | 0.000 | 0.000 | 0.223 | 1.050 | 13.7 | 150.0 | 2.00 | |
| 6°58S | 10–27 | 29.277 | 0.441 | 0.014 | 0.263 | 1.130 | 15.1 | 153.3 | 2.08 | |
| 5°00S | 10–28 | 29.114 | 1.412 | 0.024 | 0.333 | 1.770 | 15.1 | 143.8 | 3.93 | |
| 3°00S | 10–29 | 28.615 | 2.500 | 0.077 | nd | nd | 15.0 | 190.9 | 7.80 | |
| 3°03S | 10–30 | 28.595 | 2.355 | 0.073 | nd | nd | 22.2 | 281.5 | 8.05 | |
| 2°00S | 11–3 | 28.421 | 2.284 | 0.093 | 0.342 | 2.060 | 13.9 | 188.8 | 6.30 | |
| 1°00S | 11–4 | 28.231 | 2.572 | 0.156 | 0.344 | 2.280 | 10.5 | 152.3 | 5.20 | |
| 0°00 | 11–5 | 27.828 | 3.465 | 0.304 | nd | nd | 16.9 | 230.0 | 11.40 | |
| 0°01N | 11–9 | 28.218 | 1.628 | 0.221 | 0.286 | 2.160 | 17.3 | 320.2 | 11.45 | |
| 1°00N | 11–10 | 28.587 | 0.882 | 0.069 | 0.233 | 2.010 | 14.9 | 220.4 | 6.30 | |
| 4°00N | 11–11 | 28.516 | 0.811 | 0.070 | 0.233 | 1.930 | 11.6 | 169.9 | 4.95 | |
| 7°00N | 11–12 | 29.354 | 0.004 | 0.028 | 0.059 | 1.450 | 0.8 | 80.0 | 0.80 | |
| 8°00N | 11–13 | 29.278 | 0.013 | 0.003 | 0.073 | 1.500 | nd | nd | nd | |
| Latitude | mvCh | dvCh | Chl *a* | Std | n | $P_C$ | Std | n | PI | PAR $0^+$ |
| 8°02S | 0.043 | 0.052 | 0.087 | 0.002 | 2 | 0.81 | 0.15 | 5 | 8.55 | 34.7 |
| 6°58S | 0.087 | 0.083 | 0.148 | 0.006 | 2 | 1.05 | 0.10 | 16 | 6.18 | 28.2 |
| 5°00S | 0.094 | 0.074 | 0.160 | 0.008 | 2 | 1.37 | 0.08 | 5 | 8.16 | 46.2 |
| 3°00S | 0.101 | 0.056 | 0.168 | 0.015 | 2 | 1.50 | 0.08 | 5 | 9.55 | 45.1 |
| 3°03S | 0.137 | 0.117 | 0.254 | 0.010 | 5 | 1.34 | 0.04 | 5 | 5.28 | 46.2 |
| 2°00S | 0.119 | 0.076 | 0.255 | | 1 | 1.80 | 0.08 | 4 | 9.23 | 44.5 |
| 1°00S | 0.127 | 0.097 | 0.240 | 0.001 | 2 | 1.68 | 0.20 | 3 | 7.50 | 45.7 |
| 0°00 | 0.174 | 0.126 | 0.334 | 0.002 | 2 | 2.55 | 0.14 | 4 | 8.50 | 44.5 |
| 0°01N | 0.154 | 0.153 | 0.356 | | 1 | 2.09 | 0.14 | 6 | 6.80 | 36.7 |
| 1°00N | 0.128 | 0.117 | 0.276 | 0.012 | 2 | 2.27 | 0.13 | 5 | 9.28 | 42.1 |
| 4°00N | 0.116 | 0.137 | 0.266 | 0.010 | 3 | 1.50 | 0.05 | 4 | 5.93 | 41.9 |
| 7°00N | 0.028 | 0.040 | 0.093 | 0.006 | 2 | 0.39 | 0.02 | 6 | 5.79 | 40.3 |
| 8°00N | 0.026 | 0.030 | 0.062 | 0.001 | 2 | 0.34 | 0.028 | 4 | 6.04 | 40.3 |

[a]Latitude, date, temperature (°C), nutrients (μM), *Synechococcus*, *Procholorococcus*, and picoeukaryotes (cells $\mu L^{-1}$), chlorophyll *a* (fluorometer), mono- and divinyl-chlorophyll *a* (mg $m^{-3}$), primary production (mgC $m^{-3}$ $h^{-1}$), productivity index (gC gchl$a^{-1}$ $h^{-1}$) and integrated PAR $0^+$ (E $m^{-2}$ $d^{-1}$). Std = Standard deviation.

etry, seawater samples (500 mL) were filtered onto Whatman GF/F filters and extracted in 90% acetone for 12 hours in the dark at 4°C [*Neveux et al.*, 2003]. For comparison with fluorometric data, chl *a* refers to the sum of monovinyl- and divinyl-chlorophyll *a*. Samples (100 mL) for fluorometry were filtered onto GF/F filters (25-mm diameter) and extracted in 95% methanol according to the method described by *Holm-Hansen and Riemann* [1978] and modified by *Le Bouteiller et al.* [1992]. Chlorophyll *a* determinations were made within 15 to 90 min of extraction on a Turner model 112 fluorometer. Additional size-fractionated pigment samples were taken by filtering 138-mL samples first onto 3-μm polycarbonate Nuclepore filters (25 mm) with vacuum pressure <4 hPa, and then onto GF/F filters. Chl *a* was determined on each fraction by fluorometry and compared to its concentration in unfractioned samples. Most of the time, the sum of chl *a* in the fractions equalled unfractioned chl *a* within 10%.

[11] Picoplankton cells were enumerated on shipboard within two hours of collection using a FACScan flow cytometer (Becton-Dickinson) and the mean cell sizes were estimated using the flow cytometer light forward scatter according to the procedure described by *Blanchot et al.* [2001]. Cellular carbon was estimated using the statistical allometric relationships by *Verity et al.* [1992]. The conversion factors used are 470(cell volume) fgC $cell^{-1}$ for procaryotes and 433(cell volume)$^{0.863}$ fgC $cell^{-1}$ for eukaryotes. Autotrophic nanoplankton and microplankton were counted by microscopy [*Brown et al.*, 2003]. Length and width measurements were converted to biovolumes (BV; $\mu m^3$) applying appropriate geometric shapes. Cell volume to carbon conversions were based on modified *Strathmann* [1967] equations for diatoms ($\log_{10}C$ = $0.76(\log_{10}BV) - 0.352$) and nondiatom phytoplankton ($\log_{10}C = 0.94(\log_{10}BV) - 0.60$) [*Eppley et al.*, 1970].

### 2.2. Photosynthetically Available Radiation (PAR) and Euphotic Layer Depth

[12] Incident PAR (PAR $0^+$ in Table 1) was measured during incubations using a cosine-corrected Li-Cor quantameter connected to a Li-Cor integrator. In addition, two spherical sensors QSP-200L of Biospherical Instruments, one on deck and the other connected to the Sea-Bird SBE-911-plus CTD system, gave relative and absolute values of PAR in the water column.

[13] To compare the inherent capacities of light penetration in the water column at each sampling station, depth of the euphotic layer $Z_{eu}$ (1% light penetration) was calculated for every chlorophyll profile from the relationship of *Morel* [1988],

$$Z_{eu} = 38.0C^{-0.428} \quad (1)$$

with a substantial modification for C, the mean pigment content. Rather than use fluorometrically determined pigment values (i.e., chl *a* + phaeopigments), we substituted the mean active pigment content (mv-chl *a* + dv-chl *a*) measured by spectrofluorometry. This procedure gives euphotic layers several meters deeper than Morel's calculation, but slightly shallower than the euphotic layers measured in situ with our spherical quantameter.

### 2.3. Primary Production

#### 2.3.1. In Situ Experiments

[14] For three of the five days at the 3°S and 0° time series stations, seawater for in situ production measure-

ments was collected between 0400 and 0430 hours using a rosette of 12 12-L Niskin bottles. Sampling depths were every 10 m between the surface and 80 m, then 100, 120 and 150 m. Moreover, the same surface water (in reality taken between one and three meter depth) was used for in situ incubations at both 0 and 5 m. At each level, replicate samples were taken for 12- and 24-hour production experiments.

[15] New sterile 260-mL plastic bottles were filled gently using a new silicone tube washed with 0.5 N HCl and rinsed with double-distilled water. The tracer solution was prepared according to the procedure recommended by *Fitzwater et al.* [1982]. $Na_2CO_3$ was added to double-distilled water up to pH 10. $^{14}C$-$NaHCO_3$ was diluted in this water and immediately frozen in Teflon bottles. Before each experiment, one frozen aliquot of tracer solution was thawed to ambient temperature, and 0.5 or 1 mL (5 to 10 μCi of $^{14}C$) was added to each experimental bottle. For each experiment, one to several samples were inoculated with $^{14}C$ solution and immediately filtered to determine abiotic particulate $^{14}C$ incorporation. The in situ array was launched before sunrise, and picked up at about 1800. One series of replicate samples was immediately filtered, giving daytime primary production values. The other series was placed for the night in a shipboard incubator to obtain net production per day. After incubation, samples were collected on 25-mm GF/F filters using a vacuum pressure <50 hPa. Duplicate samples were fractionated onto 3-μm Nuclepore filters following the same procedure as that for pigments. At the end of filtration, filters were immediately rinsed with filtered seawater, taking the recommendations of *Goldman and Dennett* [1985] into account, and placed in 7-mL scintillation glass picovials. After addition of 100 μL of 0.5 N HCl, the vials were dried for 24 hours at 50°C before 5 mL of Ultima Gold scintillation liquid were added to each vial. $^{14}C$-$CO_2$ uptake was determined on board by using 6-min counts on a liquid scintillation counter Packard model TRI-CARB 1600-TR with a quenching correction by a $^{14}C$ internal standard. Several series of samples were counted a second time after a 24-hour delay, showing no significant difference from the first counts. For each experiment, total activity introduced into incubation samples was measured by counting several 50-μL replicates of the tracer solution in vials containing 5 mL of Instagel and 50 μL of Carbo-Sorb. Since insignificant variability of $^{14}C$ activity was detected among experiments (cv = 1.3% on 102 analyses), we used a mean value for total activity in the production calculations.

[16] Primary production rate ($P_C$, mgC $m^{-3}$ $t^{-1}$) was calculated as

$$P_C = (R - R_0)(A/Q)(1.05/t) \quad (2)$$

where R = DPM counted on GF/F filters after incubation, $R_0$ = DPM counted on GF/F filters immediately after addition of $^{14}C$, A = 24,000 mgC $m^{-3}$ = mean total inorganic carbon concentration in seawater, Q = total activity (DPM) of added $^{14}C$ carbonate solution, 1.05 is the factor for preferential fixation of $^{12}C$ over $^{14}C$, and t is the incubation time (hour or day). The productivity index (PI) is classically defined here as the amount of carbon fixed per hour normalized to initial chlorophyll *a* (gC g chl $a^{-1}$ $h^{-1}$).

### 2.3.2. On-Deck Experiments

[17] In order to compare primary production and phytoplankton biomass under varying nutrient conditions, experiments along the 8°S–8°N transect were conducted on deck under fixed optical conditions. The incubator used for that purpose was covered by a sheet of Acrylite 625-5 blue Plexiglas reducing light intensity to 30% of PAR, and was cooled with surface seawater. From three to sixteen replicate samples were taken at 20 m at stations occurring between 0200 and 0530 h, but $^{14}C$ was added to bottles just before the beginning of the experiments (0600). The profiles of density from these stations show that the 20-m depth was always included in the mixed layer recently homogenized by nocturnal convection. Hence, 20-m samples were representative of the whole mixed layer. All samples were incubated under the same light regime, close to the mean radiation available at 20-m depth, which varied during the cruise from 22 to 32% of incident PAR. The sampling depth and the light regime in these experiments correspond to the maximum of productivity index [*Cullen et al.*, 1992; *Barber et al.*, 1996] (Figure 6), providing the best sensitivity for data comparisons. All experiments were conducted between 0600 and 1800 (local time). Sample processing was similar to that of in situ experiments. During these experiments, 17 series of replicates (generally 5) were used to calculate a mean 5.7% coefficient of variability (cv) for production measurements.

## 2.4. New Production

[18] For nitrogen productivity measurements, samples were taken every 10 m between 10 and 80 m. Acid-cleaned polycarbonate bottles (1.2 L) were filled with seawater, and $^{15}N$ tracer ($K^{15}NO_3$) was added at 10 to 15% of ambient nitrate concentration. For in situ incubations, a special array was deployed before sunrise and generally recovered at midday. However, one of three experiments at the equator was incubated for the full daylight period (12 h). In that case, $^{15}N$ bottles were hung on the same array as $^{14}C$ bottles. At the end of all experiments, the incubated samples were filtered onto 25-mm precombusted GF/F filters, and the filters were dried at 50°C for 24 hours and stored with desiccant. These filters were later analyzed for $^{15}N$ enrichment and particulate N content using a Europa mass spectrometer according to the protocol described by *Raimbault et al.* [1999]. $NO_3$ uptake was calculated using an equation that takes into account the final particulate nitrogen concentration [*Dugdale and Wilkerson*, 1986],

$$P_N = (R_{PON}/R_{NO3})(t^{-1})(PON) \quad (3)$$

where $P_N$ = $NO_3$ uptake rate (mmolN $m^{-3}$ $h^{-1}$), $R_{PON}$ and $R_{NO3}$ = $^{15}N$ atom percent enrichment in the PON (final) and $NO_3$ (initial) pool, respectively, t = duration of incubation (h), and PON = particulate organic nitrogen (μM). No difference was found between hourly nitrate uptakes in one 12-hour and the two 6-hour experiments at the equator. Hence, we computed new production during the daylight hours by multiplying the measured $NO_3$ uptake per hour by 12.

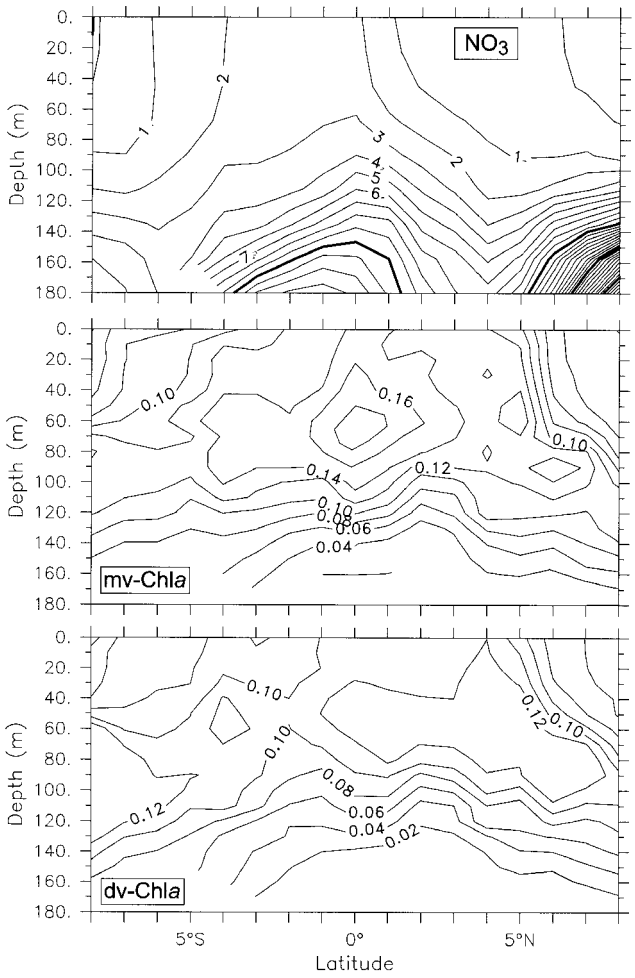


**Figure 1.** Depth distribution of nitrate (μM), monovinyl-chlorophyll *a*, and divinyl-chlorophyll *a* (mg $m^{-3}$) along the 180th meridian.

[19] The *f* ratio [*Eppley and Peterson*, 1979] was calculated for the daytime periods from new and total primary production rates values:

$$f = [P_N 6.6]/P_C \quad (4)$$

where 6.6 represents the Redfield C:N ratio for phytoplankton.

## 3. Results

### 3.1. Environmental Conditions

[20] Because of the occurrence of a cold ENSO episode (La Niña) in 1996, upwelled waters stretched westward along the equator, pushing the warm pool toward the extreme west of the Pacific. Consequently, the EBENE cruise transect along the dateline crossed a well-developed upwelling structure [*Eldin and Rodier*, 2003]. The south equatorial current (SEC) [*Wyrtki*, 1974] was observed flowing westward at about 50 cm $s^{-1}$ from 4°S to 3°N with a maximum at 1°N (up to 90 cm $s^{-1}$ at the surface). The nutrient-rich equatorial undercurrent (EUC) flowed eastward, with a maximum velocity at about 150 m centered on the equator. The maximum zonal shear between the SEC and EUC appeared near 80 m at the equator and much deeper, at about 200 m, at 3°S. As a consequence of the latitudinal difference of EUC depth and intensity, much higher nitrate and silicate concentrations were observed in the layer 100–150 m at the equator than at 3°S (Table 3). Upwelled waters extended in the upper layer from 7°S to 5°N, with clear asymmetry to the south (Figure 1), although the highest surface nitrate concentrations were measured at the equator (3.5 μM) during the first two days of the time series station. By contrast, both monovinyl-chlorophyll *a* (mv-chl *a*) and divinyl-chlorophyll *a* (dv-chl *a*) were nearly symmetrically distributed north and south of the equator, with the highest concentrations at the equator (Figure 1). Clearly, factors other than nitrate control chlorophyll distribution in the equatorial system. Indeed, although the lowest chl *a* values were found logically in nutrient-depleted waters (8°S and 7°–8°N), no clear relationship was found between chlorophyll and nutrients when data from nutrient-rich waters were considered alone. This is shown in Figure 2 where all chl *a* and $NO_3$ data from the 0–20-m surface layer are compared. When $NO_3$ equaled 30 mmol $m^{-2}$, for instance, chl *a* ranged from 3 to about 6 mg $m^{-2}$.

### 3.2. Relationship Between Production, Chlorophyll, and Picoplanktonic Population Abundances

[21] The on-deck experiments were intended to compare primary production and phytoplankton biomass under varying nutrient regimes. Environmental conditions for the transect stations are presented in Table 1. Temperature at 20 m usually exceeded 28°C, which is remarkably warm for equatorial HNLC waters. Nitrate ranged from less than 3 nM (detection limit) to 3.47 μM, and nitrite varied from 0 to 304 nM. As typical for the equatorial Pacific system, the variability of biological indexes was relatively large. Chlorophyll *a* varied by a factor of six, from 0.06 to 0.36 mg $m^{-3}$. Primary production ($P_C$) ranged from 0.34 to 2.55 mg C $m^{-3}$ $h^{-1}$ (or 0.25–1.9 mmolC $m^{-3}$ $d^{-1}$). These magnitudes are similar to those of $P_{max}$ observed in the central equatorial Pacific during the EqPac cruises in 1992 [*Barber et al.*, 1996].

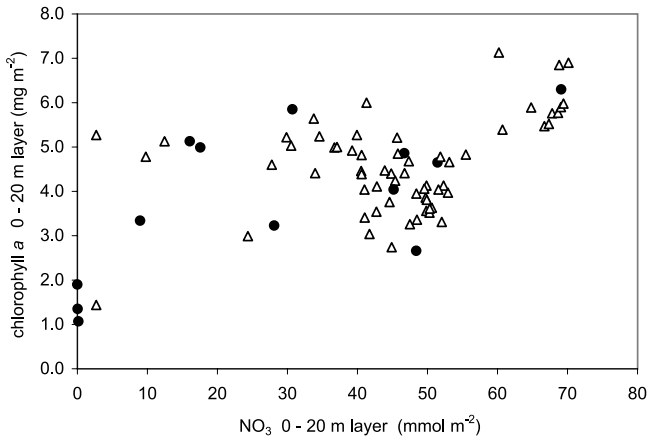


**Figure 2.** Chlorophyll *a* versus nitrate in the 0–20 m layer (all data). Solid points correspond to on-deck production measurements.

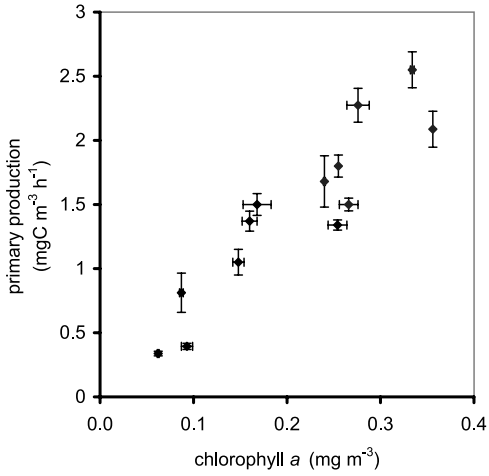


**Figure 3.** Primary production versus chlorophyll *a* at 20 m along the 180th meridian. Means ± standard deviation, 3–16 production replicate samples, and chlorophyll *a* in duplicate (see Table 1).

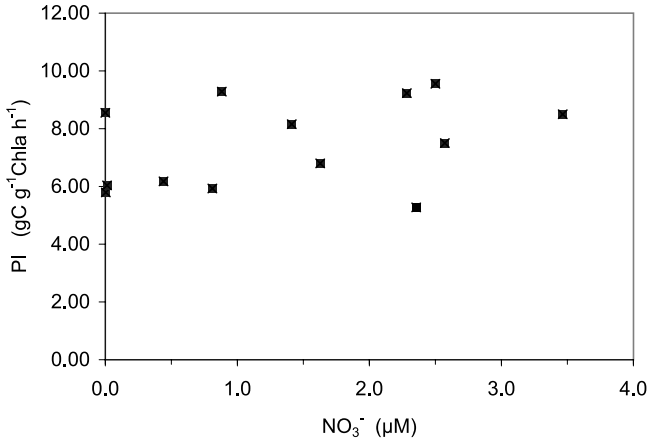


**Figure 4.** Productivity index versus nitrate concentration at 20 m along the 180th meridian.

[22] Daytime primary production rates were tightly correlated with chlorophyll *a* (Figure 3), with 80 to 83% of the $P_C$ variance explained by changes in chl *a* (Table 2). Not surprisingly, $P_C$ was also correlated to the main chl *a* constituents, monovinyl- and divinyl-chlorophyll *a*. In addition, $P_C$ was generally well related to abundances of the main three groups of picoplankton cells enumerated by flow cytometry, *Prochlorococcus*, *Synechococcus* and picoeukaryotes. In each case, a good fit to the data set was obtained by a simple linear relationship.

### 3.3. Relationship Between Productivity and Nutrient Concentration

[23] Since the *y* intercepts of $P_C$ versus chl *a* regression lines (fluorometer or spectrofluorometer analyses) were not significantly different from 0 (Table 2), the specific photosynthetic efficiency of chl *a* was nearly constant, to first approximation. Accordingly, a mean productivity index (PI), close to the slope of the regression line relating $P_C$ and chl *a* (Table 2), could be calculated from all available data. On average, PI equaled 7.0 (std = 1.6) or 7.4 (std = 1.5) gC g chl $a^{-1}$ $h^{-1}$ according to either fluorometric or spectrofluorometric chl *a* estimates. The difference between these two PI relationships was not statistically significant (Wilcoxon test).

[24] The productivity index is expected to depend on available radiation and nutrient concentration. All experiments along the transect were conducted under fixed optical conditions from dawn to dusk. Since incident radiation PAR $0^+$ varied only narrowly during the thirteen incubations (Table 1), all samples received nearly the same mean radiation and PI was not significantly correlated to PAR.

[25] No relationship was evident between PI and nutrient concentrations, in spite of a relatively large range of nutrient concentrations encountered between 8°S and 8°N. Notably, the 7 experiments conducted in waters containing >1 µM of $NO_3$ (up to 3.5 µM) did not show significantly higher PI (Mann-Whitney Test) than the 6 experiments with <1 µM of $NO_3$ (Figure 4), among which were three in extremely oligotrophic conditions (<20 nM of $NO_3$). Similarly, no significant relationship was found between PI and concentrations of phosphate or silicic acid (Table 1).

[26] PI variability is well illustrated with data from the time series at 3°S, where PI fluctuated from 9.5 to 5.3 gC g chl $a^{-1}$ $h^{-1}$ between the 29 and 30 October experiments (Table 1). These values are close to the largest and the lowest PIs measured along the entire transect. Why PI changed so dramatically from one day to the next is not clear. The production variance was low in both cases (cv = 5.7 and 3.0%, respectively, for 5 replicates), and the experimental conditions were rigorously similar, with the same mean incident radiation, temperature, salinity, current advection and nutrient concentrations (Table 1). Therefore,

**Table 2.** Coefficients of the Linear Regression of Primary Production Versus Total Chlorophyll *a* (Measured by Fluorometry and by Spectrofluorometry), Mono- and Divinyl-Chlorophyll *a* and Cells Enumerated by Flow Cytometry[a]

| | | | Model II | | Model I | | | |
|---|---|---|---|---|---|---|---|---|
| | r | $r^2$ | Slope | $y_0$ | Slope | $y_0$ | t ($y_0$) | $P_C$ |
| Chl *a* (fluo) | 0.913 | 0.83 | 7.08 | −0.036 | 6.47 | 0.095 | 0.482 | 0.64 |
| Chl *a* (spect) | 0.892 | 0.80 | 8.12 | −0.120 | 7.25 | 0.049 | 0.211 | 0.84 |
| Mv-chl *a* | 0.933 | 0.87 | 14.4 | −0.050 | 13.5 | 0.055 | | |
| Dv-chl *a* | 0.778 | 0.61 | 17.3 | −0.099 | 13.4 | 0.242 | | |
| Syn. | 0.664 | 0.44 | 0.108 | 0.049 | 0.072 | 0.510 | | |
| Proc. | 0.701 | 0.49 | 0.010 | −0.483 | 0.007 | 0.079 | | |
| Picoeuk. | 0.859 | 0.74 | 0.186 | 0.419 | 0.160 | 0.553 | | |

[a]Results of tests on the significance of the y intercept for $P_C$ versus chl *a* [*Snedecor and Cochran*, 1967] show that in both cases, y intercept is not significantly different from 0. Standard regression (model I) and geometric mean regression (model II). Thirteen on-deck experiments.

**Table 3.** Means (Standard Deviations) of Nutrient Concentrations (μM; n = 3), Mono- and Divinyl-Chlorophyll *a* (mg $m^{-3}$), *Prochlorococcus*, *Synechococcus*, and Picoeukaryotes (cells $\mu L^{-1}$) in Samples Used for in Situ Primary Production Experiments[a]

| Depth | $NO_3$ | $Si(OH)_4$ | $NH_4$ | Mv-chl *a* | Dv-chl | Proc | Syn | Pico |
|---|---|---|---|---|---|---|---|---|
| | | | | *3°S* | | | | |
| 0 | 2.34 (0.14) | 1.94 (0.23) | 0.128 (0.086) | 0.103 (0.010) | 0.082 (0.010) | 240 (23) | 17.9 (2.2) | 7.8 (1.1) |
| 10 | | | 0.094 (0.073) | 0.110 (0.006) | 0.081 (0.013) | 236 (19) | 18.0 (2.3) | 8.0 (1.1) |
| 20 | 2.34 (0.17) | 1.83 (0.24) | 0.062 (0.043) | 0.116 (0.006) | 0.091 (0.006) | 256 (6) | 18.9 (2.0) | 8.2 (0.4) |
| 30 | | | 0.069 (0.046) | 0.138 (0.007) | 0.108 (0.005) | 280 (28) | 21.3 (2.0) | 8.9 (0.6) |
| 40 | 2.40 (0.22) | 1.77 (0.23) | 0.088 (0.071) | 0.152 (0.016) | 0.122 (0.012) | 260 (48) | 20.9 (5.0) | 8.5 (1.3) |
| 50 | | | | 0.154 (0.019) | 0.120 (0.016) | 221 (35) | 18.7 (3.5) | 7.4 (0.7) |
| 60 | 2.47 (0.26) | 1.74 (0.25) | 0.144 (0.079) | 0.143 (0.022) | 0.116 (0.022) | 178 (27) | 16.0 (2.4) | 6.3 (0.3) |
| 70 | 2.54 (0.30) | 1.76 (0.24) | 0.220 (0.132) | 0.140 (0.022) | 0.112 (0.033) | 139 (31) | 12.6 (3.4) | 5.3 (0.6) |
| 80 | 2.55 (0.26) | 1.74 (0.25) | 0.243 (0.087) | 0.130 (0.023) | 0.099 (0.026) | 99 (39) | 9.5 (3.8) | 4.1 (1.3) |
| 90 | 2.64 (0.35) | 1.75 (0.28) | 0.318 (0.143) | | | | | |
| 100 | 2.89 (0.33) | 1.82 (0.24) | 0.455 (0.190) | 0.094 (0.020) | 0.059 (0.025) | 39 (12) | 4.0 (2.0) | 2.1 (0.6) |
| 110 | 3.15 (0.37) | 1.91 (0.30) | 0.508 (0.197) | | | | | |
| 120 | 3.27 (0.53) | 1.88 (0.25) | 0.554 (0.279) | 0.083 (0.005) | 0.047 (0.003) | 20 (2) | 0.6 (0.4) | 1.2 (0.1) |
| 130 | 3.55 (0.30) | 1.88 (0.25) | 0.343 (0.309) | | | | | |
| 140 | 4.58 (0.09) | 1.69 (0.32) | 0.112 (0.189) | | | | | |
| 150 | 6.37 (0.80) | 1.78 (0.43) | 0.020 (0.012) | 0.042 (0.007) | 0.028 (0.001) | 10 (0.5) | 0.0 (0.0) | 0.4 (0.1) |
| | | | | *Equator* | | | | |
| 0 | 1.79 (0.15) | 2.18 (0.16) | 0.057 (0.045) | 0.129 (0.018) | 0.112 (0.011) | 241 (9) | 14.4 (1.4) | 7.9 (0.7) |
| 10 | | | 0.047 (0.040) | 0.126 (0.006) | 0.115 (0.015) | 235 (10) | 14.1 (1.3) | 7.4 (1.1) |
| 20 | 1.92 (0.16) | 2.12 (0.14) | 0.042 (0.036) | 0.135 (0.012) | 0.119 (0.012) | 240 (28) | 13.7 (1.9) | 7.3 (1.2) |
| 30 | | | 0.046 (0.030) | 0.140 (0.006) | 0.119 (0.006) | 233 (34) | 13.5 (2.3) | 7.2 (0.6) |
| 40 | 2.22 (0.14) | 2.13 (0.11) | 0.052 (0.027) | 0.152 (0.002) | 0.121 (0.007) | 222 (47) | 12.5 (3.0) | 7.3 (1.3) |
| 50 | | | | 0.154 (0.011) | 0.128 (0.012) | 191 (39) | 11.2 (2.8) | 6.8 (0.9) |
| 60 | 2.74 (0.08) | 2.18 (0.13) | 0.073 (0.046) | 0.165 (0.013) | 0.122 (0.010) | 165 (28) | 9.8 (2.4) | 5.9 (1.5) |
| 70 | 2.92 (0.09) | 2.19 (0.11) | | 0.172 (0.015) | 0.121 (0.007) | 142 (23) | 9.5 (2.5) | 6.3 (1.5) |
| 80 | 3.25 (0.19) | 2.22 (0.11) | 0.080 (0.056) | 0.175 (0.025) | 0.114 (0.021) | 117 (23) | 7.4 (2.1) | 5.4 (1.6) |
| 90 | 3.56 (0.12) | 2.25 (0.06) | 0.082 (0.059) | | | | | |
| 100 | 4.19 (0.30) | 2.33 (0.00) | 0.060 (0.046) | 0.162 (0.011) | 0.096 (0.004) | 66 (13) | 4.2 (0.8) | 3.8 (1.0) |
| 110 | 5.31 (0.82) | 2.61 (0.27) | 0.030 (0.038) | | | | | |
| 120 | 7.40 (1.11) | 2.98 (0.36) | 0.016 (0.020) | 0.138 | 0.069 | 31 (16) | 1 (1.2) | 1.6 (1.1) |
| 130 | 8.66 (0.70) | 3.49 (0.70) | 0.010 (0.013) | | | | | |
| 140 | 10.16 (0.48) | 4.90 (0.07) | 0.010 (0.012) | | | | | |
| 150 | 11.16 (0.10) | 5.80 (0.90) | | 0.064 | 0.036 | | | |

[a]Mean $NH_4$ values calculated from 30 and 25 profiles at 3°S and 0°, respectively.

if not because of a hypothetical change of iron availability, such variability might be inherent to field process studies, involving bottle incubations under varying light regimes with complex natural communities of closely interdependent autotrophic and heterotrophic organisms. Alternatively, the variability could be due to differences in C/chl *a* ratio or growth rate (see below).

### 3.4. Relationship Between Productivity and Depth

[27] While the on-deck experiments conducted from 8°S to 8°N relate to the photosynthetic capacity of mixed layer phytoplankton, in situ experiments at the two time series stations allow us to determine productivity for the total euphotic zone. During these latter experiments, surface nitrate concentration was slightly lower at 0° than at 3°S, but much higher at depth, especially between 100 and 150 m (Table 3). Ammonium was much higher at 3°S (Table 3), suggesting stronger remineralization processes than at the equator [*Eldin and Rodier*, 2003]. However, silicic acid, $Si(OH)_4$, was clearly and significantly higher throughout the water column at the equator than at 3°S (Table 3). Although chl *a* fractionations on 3-μm Nuclepore filters did not show any difference between the two stations (Figure 5), biogenic silica concentration was >threefold higher at 0° than at 3°S, increasing from 2.26 to 7.61 mmolSi $m^{-2}$ in the top 100 m [*Leynaert et al.*, 2001]. This dissimilarity could reflect better growth conditions for siliceous organisms on the equator due to the strong divergence bringing macronutrients and micronutrients into the mixed layer. The lack of any obvious change of size structure may be explained by the relative paucity of the siliceous organisms compared to other microphytoplankton and nanophytoplankton [*Brown et al.*, 2003], or if diatoms and silicoflagellates were sufficiently narrow to pass through the 3-μm filters.

[28] Chlorophyll in near-surface waters was nearly 25% higher at 0° than at 3°S (Figure 6). chl *a* vertical profiles exhibited a smooth deep maximum at about 60 m, a pattern quite typical of the equatorial Pacific HNLC system [*Chavez et al.*, 1991; *Barber et al.*, 1996]. The three groups of cells enumerated by flow cytometry showed maximal abundances in the upper layer at 3°S and on the equator as well, with relatively comparable patterns of decrease with depth (Table 3).

[29] Closely following the concentration difference of chl *a*, production appeared to be about 25% higher at 0° than at 3°S in the surface layer (Figure 6). However, reflecting the same chl *a* size structure, primary production predominated in the <3-μm size class throughout the euphotic zones at the two sites (Figure 5). Production maxima ($P_{max}$) were typically observed at 20 m in both 12- and 24-hour incubations, with mean values of 12.0 (3°S) and 15.7 mgC $m^{-3}$ $d^{-1}$ (0°). In the water column, 48% (3°S) and 55% (0°) of integrated production were measured in the top 30 m, which contained only 23% of

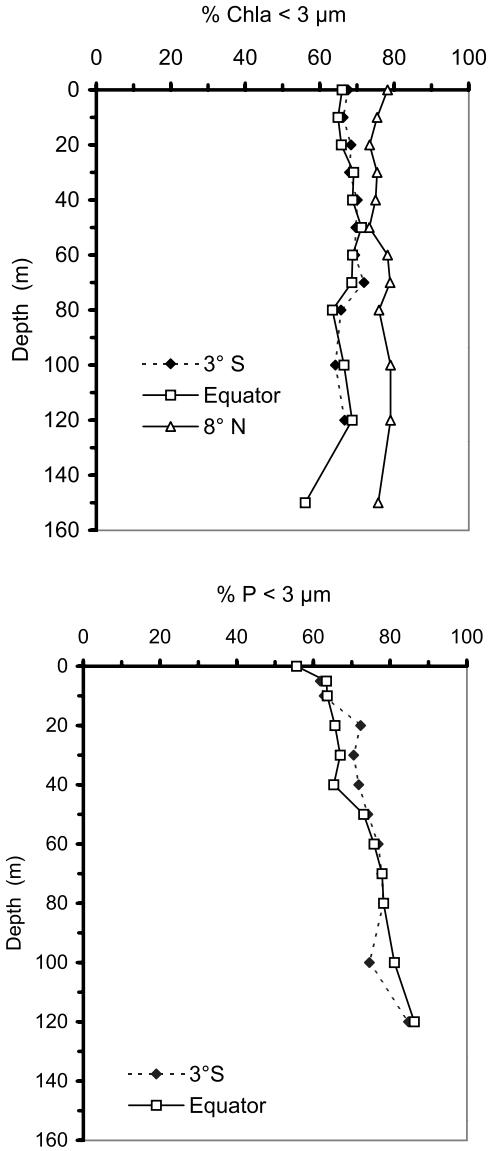


**Figure 5.** (top) Chlorophyll *a* size distribution in HNLC (3°S and 0°) and oligotrophic (8°N) conditions. On average, chl *a* < 3µm = 68.4% (3°S), 67.2% (0°), and 77.6% (8°N). (bottom) Size distribution of in situ primary production (3°S and 0°). On average, $P_C$ < 3µm = 71% (3°S) and 69% (0°).

integrated chl *a* on average. Conversely, the deep 60–150 m layer, containing 50 to 57% of chl *a*, accounted for only 10 to 16% of total production. At 100 m, phytoplankton appeared quasi-nonproductive (Figure 6).

[30] During the six 12-hour in situ experiments (sunrise to sunset) at 3°S and 0°, production rates ranged between 900 and 1070 mgC $m^{-2}$ $d^{-1}$. Rate differences between 12- and 24-hour incubations were consistent with a mean nocturnal loss of 25.7% of daily $^{14}C$ uptake, which is quite close to the mean value (24%) found by *Laws et al.* [1989] in the North Pacific central gyre. The daily production rates ($P_C$ = 702 and 774 mgC $m^{-2}$ $d^{-1}$ at 3°S and the equator, respectively) were relatively low, appearing at the lower limit of values measured in situ in the western Pacific HNLC region. For example, during the Zonal Flux cruise (April 1996), $P_C$ estimates at 165°E (2°N–2°S) ranged between 667 and 1196 mgC $m^{-2}$ $d^{-1}$ (3 production profiles), and a mean value of 1094 mgC $m^{-2}$ $d^{-1}$ was obtained along the equator from 165°E to 170°W (4 profiles) [*Le Borgne et al.*, 1999].

[31] The productivity index was maximal between 5 and 20 m (Figure 6), in good agreement with previous in situ experiments in equatorial regions [*Le Bouteiller and Herbland*, 1984; *Cullen et al.*, 1992; *Barber et al.*, 1996]. The maximal PI for in situ incubations was close to or slightly lower than the mean value for 20-m samples under simulated in situ conditions, a result that confirms that on deck measurements were suitable for assessing production rates under optimal conditions. Depth distributions of PI from 12- and 24-hour experiments did not differ much from one day to another (mean cv = 15%, six experiments). Below the maximum, PI generally decreased more rapidly at 0° than at 3°S. This may be explained by differences in light penetration due to less phytoplanktonic pigment biomass at 3°S. Euphotic zone depth (1% light depth) was slightly deeper (82 ± 7 m versus 75 ± 5 m) at 3°S that the equator. Higher levels of PAR were thus available throughout the euphotic layer at 3°S, explaining higher PI at similar depths. To take such light differences into account, PI may be considered a function of $Z/Z_{eu}$ instead of Z ($Z_{eu}$ calculated as in section 2.2). Using this approach, Figure 6 shows that distributions of PI versus $Z/Z_{eu}$ at 3°S and 0° were indistinguishable. A similar pattern was obtained for the 24-hour in situ incubations.

### 3.5. Primary Production Along the 180° Meridian

[32] Given the uniformity of PI from 8°S to 8°N, the lack of a relationship between $P_C$ and mixed layer nutrients and the similarities of PI versus $Z/Z_{eu}$ at 3°S and 0°, one may assume a strong dependency of primary production on concentration of photosynthetic pigments. Accordingly, we estimated daily primary production ($P_C$) at every depth from chl *a* (mv-chl *a* + dv-chl *a*) using the mean PI (gC gchl $a^{-1}$ $d^{-1}$) versus $Z/Z_{eu}$ relationship (Figure 6). Depths of the euphotic layer ($Z_{eu}$), calculated from equation (1), ranged from 58 m at the equator to 103 m at 8°N, which is probably close to the maximum range in the region. The distribution of calculated primary production was monotonous and almost symmetrical relative to the equator, with a slight maximum on the equator (814 mgC $m^{-2}$ $d^{-1}$) and minimal values at northern and southern edges of the transect (Figure 7). The lowest production was 385 mgC $m^{-2}$ $d^{-1}$ at 8°N, corresponding to the lowest value measured in simulated in situ conditions (Table 1). The mean $P_C$ in the upwelled waters (7°S to 5°N) equaled 713 mgC $m^{-2}$ $d^{-1}$ (n = 13; std = 69). On average, production varied twofold between mesotrophic HNLC and oligotrophic waters. Averaged over the 7°S – 5°N meridional band, production at 180° was very consistent with values measured at 140°W by *Barber et al.* [1996], who found a mean $P_C$ of 888 mgC $m^{-2}$ $d^{-1}$ between 5°N and 5°S and 624 mgC $m^{-2}$ $d^{-1}$ from 10°N to 10°S.

[33] Since the chlorophyll data for the production calculations had been collected along the transect at varying times of the day or night, diel variations in pigment concentration can affect the estimated value of $P_C$. Diel changes of chlorophyll were determined during the two time

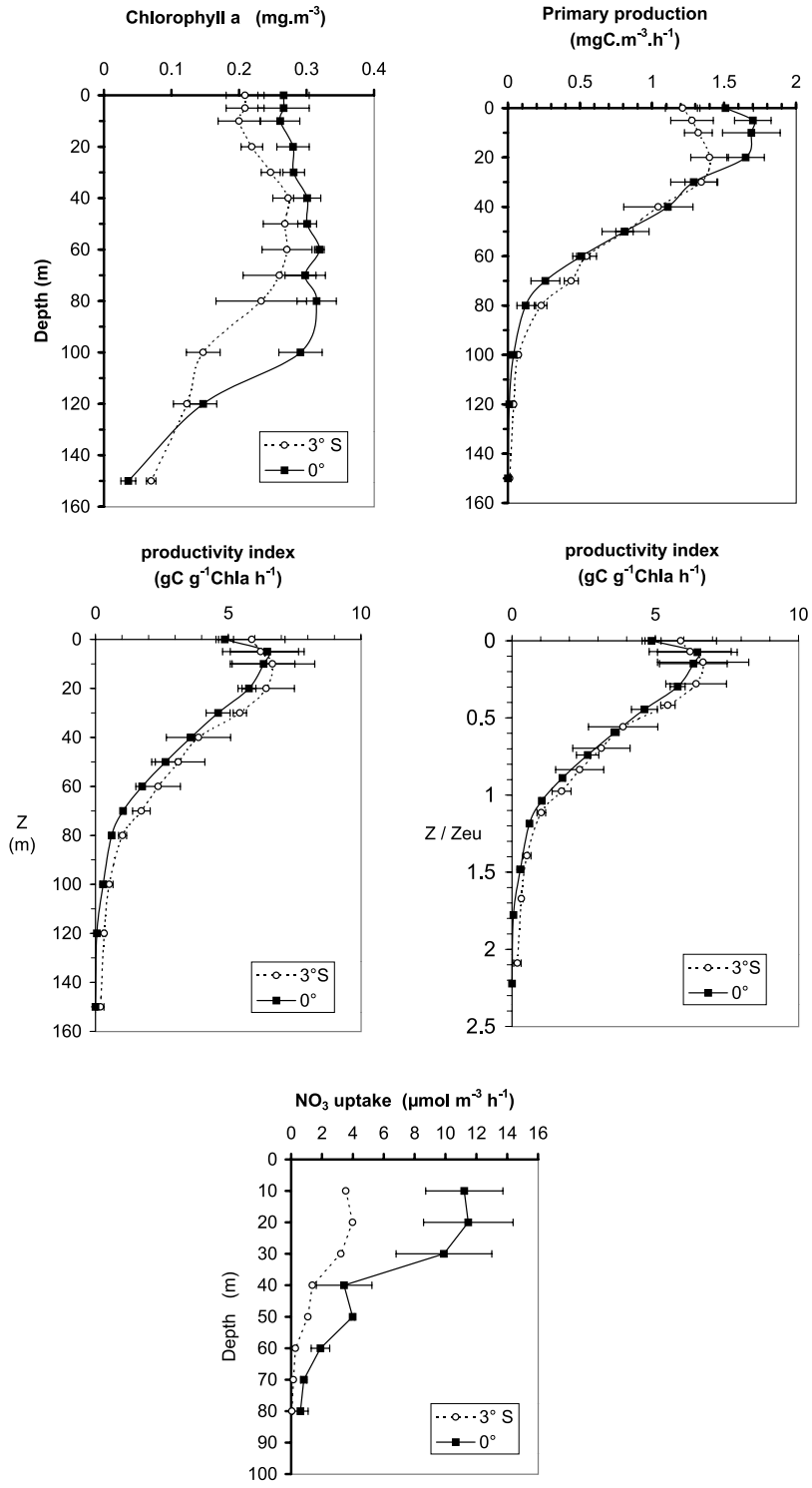


**Figure 6.** Chl *a*, $P_C$, PI, and nitrate uptake versus depth and PI versus Z/Zeu. Means ± standard deviation of three in situ experiments at 0° and 3°S.

series stations at 3°S and the equator by an intensive sampling effort (49 hourly stations followed by 16 stations every 3 h, with pigment sampling at every 10 m) [*Neveux et al.*, 2003]. Minimal concentrations of chlorophyll in the water column occurred around midnight and maximal values at stations near midday, with a relatively weak, but significant, mean amplitude of 1.16 (0°) and 1.08 (3°S). Clearly, the amplitude of pigment diel variations was too small to significantly affect the production values estimated from chlorophyll data collected between 8°S and 8°N (Figure 7).

### 3.6. New Production

[34] Daytime new production ($P_N$) measured in situ as uptake of $^{15}N$-$NO_3$ increased from 1.8 mmolN $m^{-2}$ 12 $h^{-1}$ at 3°S to 4.7 mmolN $m^{-2}$ 12 $h^{-1}$ at the equator (Figure 6).

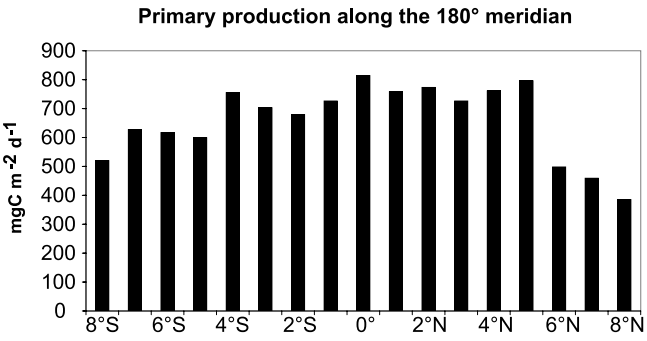


**Figure 7.** Distribution of primary production ($P_C$) estimated along the 180° meridian.

Values of daily $P_N$ reported previously for the central equatorial Pacific varied on the whole from 0.7 to 4.42 mmolN $m^{-2}$ $d^{-1}$ [*Dugdale et al.*, 1992; *Peña et al.*, 1992; *McCarthy et al.*, 1992; *Rodier and Le Borgne*, 1997; *Raimbault et al.*, 1999; *Aufdenkampe et al.*, 2002]. Thus the rate of new production found at 3°S was typical of the equatorial Pacific, whereas that at the equator was close to the highest reported value. The *f* ratio calculated for the daytime period was 0.15 at 3°S, similar to most values estimated in the central equatorial Pacific [*McCarthy et al.*, 1996, Table 1; *Raimbault et al.*, 1999]. Regenerated production strongly predominated at 3°S, which was consistent with relatively high $NH_4$ availability observed in the water column (16.4 mmol $m^{-2}$ in the 0–100-m layer; Table 3). By contrast, the *f* ratio was 0.37 at the equator where $NH_4$ was poor (6.2 mmol $m^{-2}$). This ratio was similar to the highest value found at 150°W during a zonal transect [*Aufdenkampe et al.*, 2002], suggesting that we sampled a particularly efficient system. This statement is also supported by parallel measurements of biogenic silica production uptake in our in situ experiments [*Leynaert et al.*, 2001] showing that $Si(0H)_4$ uptake rate increased from 0.33 to 2.58 mmolSi $m^{-2}$ $d^{-1}$ between 3°S and the equator.

[35] Uptake rates of nitrate and silicate have seldom been measured at the same time. Considering the key role of diatoms in the export of organic carbon to the deep sea, and thus in the biological pumping of $CO_2$ [*Buesseler*, 1998; *Kemp et al.*, 1999; *Ragueneau et al.*, 2000], it is interesting to estimate, from our simultaneous in situ measurements, the contribution of diatoms to new production. Taking a Si:N uptake ratio for diatoms of 1.05 [*Brzezinski*, 1985] and assuming that the N requirements of diatoms are fully met by $NO_3$ uptake [*Dortch*, 1990], the $NO_3$ and $Si(OH)_4$ production rates indicate that about 22% and 69% of new production at 3°S and 0°, respectively, could be attributable to diatoms and other siliceous organisms. Even if overestimated because of $NH_4$ consumption by diatoms, this increase in the diatom contribution to new production seems significant and would be linked to latitudinal variations in the rate of supply of nutrients (particularly silicic acid and iron) to the surface layer. Kinetics studies of silicic acid uptake [*Leynaert et al.*, 2001] have shown that $K_s$ values (1.6 and 2.4 μM of $Si(OH)_4$, at 3°S and at the equator, respectively) were close to the ambient silicic acid concentrations (Table 3), whereas $V_{max}$ was about twofold higher at the equator (0.052 $h^{-1}$) than at 3°S (0.028 $h^{-1}$). These variations of the kinetic parameters suggest either a change in the composition of diatom assemblages, or an adaptation of diatom metabolism in response to limitation by some other (micro)nutrient.

[36] Between 3°S and the core of the equatorial upwelling, the striking similarity of PIs and plankton size structures, and the slight variations in biomass and primary production mask a great functional discrepancy due to changes in the dynamics of diatom populations. These latitudinal changes have conspicuous effects upon new production expressed both in terms of silicic and nitrate uptake rates.

## 4. Discussion

### 4.1. Variability of the Productivity Index

#### 4.1.1. PI and Nutrients

[37] The lack of correlation between the productivity index and nutrient concentrations is perhaps surprising since one may intuitively expect the specific activity of chlorophyll to be related to nutrient availability. PI has even been linked to the degree of growth limitation by nutrients [*Curl and Small*, 1965; *Thomas*, 1970]. For example, *Curl and Small* [1965] suggested that a PI of 0–3 gC gchl $a^{-1}$ $h^{-1}$ would indicate nutrient depletion, ratios between 3 and 5 would indicate borderline nutrient deficiency, and between 5 and 10, nutrient-replete waters. By these criteria, all of stations along the EBENE transect gradient from HNLC to oligotrophic waters would be considered nutrient replete.

[38] In previous studies in the central Pacific along 140°W, *Lindley et al.* [1995] and *Barber et al.* [1996] found a PI nutrient dependency, with the index varying threefold from oligotrophic waters north and south of the EqPac transects through mesotrophic HNLC waters enriched by the equatorial divergence. Nonetheless, such relations between PI and nutrients have not often been observed in the equatorial zonal band 10°N–10°S. At 4°W in the equatorial Atlantic, *Herbland and Le Bouteiller* [1983] found higher PI values in the nitrate-depleted mixed layer rather than nutrient-rich waters. Moreover, from 54 in situ primary production experiments over four cruises in the central Atlantic, PI profiles were similar in and out of the upwelling system, and with or without nitrate in the mixed layer [*Le Bouteiller and Herbland*, 1984]. Similar findings were noted by *Navarette* [1998] for two time series stations in the equatorial Pacific at 167°E in the "warm pool" (top of the nitracline = 90 m) and at 150°W in the HNLC region (3 μM of surface $NO_3$). From 12-hour daytime in situ incubations, her mean PI values at 20 m were very close in both situations, 8.7 ± 1.0 (n = 3) at 167°E versus 8.9 ± 1.1 gC gchl $a^{-1}$ $h^{-1}$ (n = 7) at 150°W.

[39] High PIs, around 10 gC gchl $a^{-1}$ $h^{-1}$, have been also observed in very oligotrophic waters of the Pacific Ocean [*Laws et al.*, 1984, 1987, 1990]. *Karl et al.* [1998] reviewed recent literature values for PI in near-surface waters of the North Pacific Central Gyre and showed a large variability, between 3.5 and 10, and up to 14. A mean of 6.0 ± 0.7 gC gchl $a^{-1}$ $h^{-1}$ was found for monthly in situ incubations at station ALOHA for the 1990–1997 period. Given these many examples of high PIs in tropical and subtropical oligotrophic waters, the estimates of 7 or 8 gC gchl $a^{-1}$ $h^{-1}$ reported here are clearly not atypical for nutrient-depleted waters.

**Table 4.** Carbon Content (Co, mgC $m^{-3}$) of Total Phytoplankton, C:chl *a* Ratio in mg(PhytoC) mg chl $a^{-1}$, $P_C$ in (mgC $m^{-3}$ $h^{-1}$)12 From On-Deck Experiments, and Phytoplankton Community Growth Rate ($\mu$, $d^{-1}$)[a]

| Latitude | Co | C:chl *a* | $P_C$ | $\mu$ |
|---|---|---|---|---|
| 8°S | 17.7 | 155 | 9.7 | 0.43 |
| 7°S | 13.0 | 79 | 12.6 | 0.68 |
| 6°S | 16.7 | 107 | | |
| 5°S | 19.0 | 121 | 16.4 | 0.62 |
| 4°S | 22.7 | 94 | | |
| 3°S | 26.1 | 118 | 17.0 | 0.50 |
| 2°S | 23.3 | 114 | 21.6 | 0.66 |
| 1°S | 30.6 | 131 | 20.2 | 0.51 |
| 0° | 29.8 | 110 | 27.8 | 0.66 |
| 1°N | 27.5 | 107 | 27.2 | 0.69 |
| 2°N | 17.2 | 65 | | |
| 3°N | 20.7 | 85 | | |
| 4°N | 22.1 | 88 | 18.0 | 0.60 |
| 5°N | 18.5 | 80 | | |
| 6°N | 7.5 | 92 | | |
| 7°N | 7.4 | 108 | 4.7 | 0.49 |
| 8°N | 5.9 | 112 | 4.1 | 0.53 |

[a]From *Brown et al.* [2003].

Even compared to active upwelling conditions at the equator, the PI at nutrient poor stations was not substantially reduced on average. This implies that the equatorial Pacific is an oceanic province within which the productivity index at mean irradiance might be considered relatively constant [*Platt et al.*, 1992; *Cullen et al.*, 1992].

#### 4.1.2. PI, Growth Rate, and C:chl *a*

[40] In considering the lack of a strong latitudinal variation of PI in the present study, it is important to recognize how the index may vary independently of nutrients, especially in systems of relatively low physical variability. According to *Laws and Wong* [1978], PI may be written as the product of the fractional rate of increase of cellular C and the C:chl *a* ratio,

$$\mathrm{PI} = (1/\mathrm{C}\ d\mathrm{C}/dt)(\mathrm{C} : \mathrm{chl}\ a) \tag{5}$$

where C is the carbon cell content in phytoplankton. On an average, the term (1/C dC/dt) can be approximated by the growth rate ($\mu$). If C:chl *a* is independent of $\mu$, then PI would indeed be positively correlated with growth rate, and would likely vary systematically across any environmental gradient that affects $\mu$. However, if C:chl *a* and $\mu$ are inversely correlated, the product of the two terms, which gives the PI estimate, would be independent of $\mu$ [*Laws and Wong*, 1978].

[41] While processes leading to perfectly offsetting variations in $\mu$ and C:chl *a* would be difficult to imagine, there is ample reason to expect at least some compensatory change in these parameters with fluctuations in the availability of iron in the equatorial Pacific. During the IronEx II fertilization experiment, for example, *Landry et al.* [2000a, 2000b] documented a twofold decrease in the estimated C:chl *a* ratio of the phytoplankton community over a 5-day period in which growth rate approximately doubled. These responses were likely due, in part, to changes in community composition as diatoms increased from rare initially to the biomass dominants. Nonetheless, compositional changes are also characteristic of the difference between relatively weak and strong upwelling conditions (iron input) at the equator [e.g., *Landry et al.*, 1997], and thus they reflect one dimension of the natural community response to changing growth substrate concentration. In the IronEx II example, however, there is also evidence for decreasing C:chl *a* ratios of specific groups, such as prymnesiophytes and dinoflagellates [*Landry et al.*, 2000a]. Moreover, on the basis of flow cytometric assessments, *Cavender-Bares et al.* [1999] estimated a 50% increase in the pigment fluorescence of *Prochlorococcus* relative to cell biovolume, decreasing its C:chl *a*, while contemporaneous estimates of *Prochlorococcus* growth rate showed a 60% increase in response to added iron [*Mann and Chisholm*, 2000]. The above results are consistent with the negative relationship observed between cellular C:chl *a* and iron concentration in iron-deficient laboratory cultures of phytoplankton [*Sunda and Huntsman*, 1997]. It is only a modest logical leap to expect that variations in iron supply, reflecting distance from the upwelling source, could simultaneously alter both the C:chl *a* ratio and the growth rate of phytoplankton in a manner that maintains PI within some relatively high and narrow range.

[42] We examined the possibility of compensatory variations in C:chl *a* and $\mu$ using two independent components of the EBENE data. The first approach is based on assessments of phytoplankton community carbon and C:chl *a* from microscopy and flow cytometry, using standard conversions from cells and biovolumes to carbon (section 2.1). Mixed layer estimates of C:chl *a* by this approach fall in the range of 65 to 155, with higher values tending to the southern side of the transect and lower values to the north (Table 4). At C:chl *a* = 110, the equatorial time series station falls on the decreasing trend between southern and northern stations and slightly lower than the 118 estimate at 3°S. From the initial phytoplankton carbon concentrations ($C_o$, mgC $m^{-3}$), we can also compute a first-order approximation of growth rate ($\mu$; $d^{-1}$) as:

$$\mu = \ln((\mathrm{C_o} + 12{*}\mathrm{P_C})/\mathrm{C_o}) \tag{6}$$

where $P_C$ is the hourly rate of carbon fixation and time is understood as one day. According to these calculations, growth rate estimates at 20 m vary somewhat less than a factor of two (0.43 to 0.69 $d^{-1}$) along the transect, with low values interspersed throughout but tending toward the northern and southern extremes (Table 4). The mean growth rate estimate for the equatorial time series station (0.66 $d^{-1}$) is higher than that computed at 3°S (0.50 $d^{-1}$). For these data, which relate to the full phytoplankton assemblages at each of the stations, the relationship between $\mu$ and C:chl *a* is negative (Figure 8a).

[43] Although results of the community based comparisons of C:chl *a* and $\mu$ are consistent with expected compensatory changes that suppress variations in PI, part of the noise in the observed relationship may be due to the fact that stock and rate assessments were not always made from the same water sampling bottles. To further examine this phenomenon, we consider only that component of the community (<3-$\mu$m cells) that were routinely quantified for each $^{14}C$ uptake incubation. Mean cell size and carbon content of *Prochlorococcus*, *Synechococcus* and picoeukaryotic cells were computed using flow cytometry data (section 2.1). Chlorophyll values and production rates were

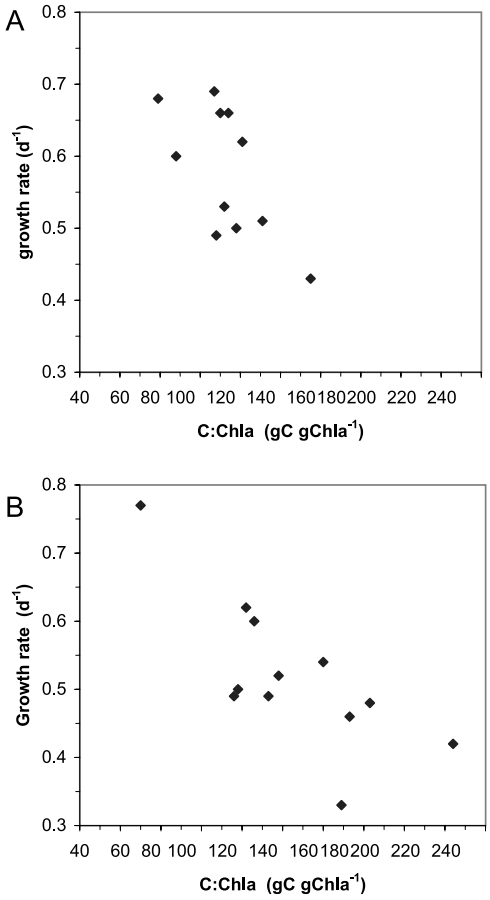


**Figure 8.** (a) Growth rate ($d^{-1}$) versus C:chl *a* (gC gchl $a^{-1}$) of the total phytoplankton community at 20 m along the transect (180°). Spearman's rank correlation coefficient = −0.62, P < 0.05. (b) Growth rate ($d^{-1}$) versus C:chl *a* (gC gchl $a^{-1}$) of the <3 μm size fraction at 20 m (180°). Spearman's rank correlation coefficient = −0.66, P < 0.02.

determined for this size class by routine size fractionation at 3 μm (Figure 5), and growth rates were computed as above from equation (6). For this component of the community, C:chl *a* varied around a mean value of 144, and growth rate averaged 0.52 $d^{-1}$ (Table 5). Because of uncertainties in cell size estimates from flow cytometry, especially in the nitrate-depleted mixed layer [*Blanchot et al.*, 2001], carbon contents are only approximate and computed values of C:chl *a* and μ have to be taken with caution. Nevertheless, they also appear to be inversely related (Figure 8b). Furthermore, the highest C:chl *a* ratio and the lowest μ of the data set correspond, respectively, to the first and second experiments at 3°S, which could partly explain the PI variability discussed in section 3.3.

[44] While growth rate estimates for the <3-μm fraction showed no significant relationship to mixed layer nitrate availability along the transect (Table 5), community-based estimates were lowest, averaging 0.48 $d^{-1}$, at the 3 stations (8°S, 7°N, and 8°N) where nitrate was essentially at the detection level (Table 4). For the EqPac transect studies between 12°N and 12°S at 140°W, *Liu et al.* [1999] also found higher growth rates (up to 0.64 $d^{-1}$ at 1°S) for *Prochlorococcus* during active upwelling in the HNLC region versus 0.36–0.5 $d^{-1}$ at oligotrophic stations. In addition, *Prochlorococcus* growth estimates decreased at the equator during El Niño conditions. In apparent contradiction to these intuitively reasonable observations, *Claustre et al.* [1999] reported that growth rates of phytoplankton along 150°W were higher in the nitrate-depleted euphotic layer at 16°S (0.63 ± 0.07 $d^{-1}$) than in HNLC waters at 5°S (0.47 ± 0.13 $d^{-1}$). These growth rate inferences were made from daily fluctuations in particle attenuation, however, and could be sensitive to the assumptions used to account for daily cycles in growth and grazing in the two regions.

[45] The photoadaptative reaction of phytoplankton to light is an important process known to influence C:chl *a*. The ratio is expected to be low at depth and high in near-surface waters. During the present cruise, water samples for primary production measurements were collected from one to four hours before sunrise, and the 20-m depth was systematically in the mixed layer homogenized by nocturnal convection. This homogeneous layer varied in thickness from 20 to 100 m along the transect, with a median value of 55 m. During stratification on the previous day, these cells photoadaptated according to their positions in the vertical radiative gradient. During nocturnal convection, the cells were mixed up and down so that a mixture of cells adapted to the range of radiative levels proportional to the thickness of the homogeneous layer appeared progressively in the upper layer. Consequently, only slight differences of photoadaptation, hence mean C:chl *a*, should have existed between samples collected at different stations. The observed variability at the presunrise sampling stations, from 65 to 155, may reflect inherent sampling and analytical error for microscopical assessments of biomass, or some combination of factors relating to community composition or previous light history (incident light or mean depth of the mixed layer).

[46] To ascertain the depth dependencies of μ and C:chl *a* for the <3-μm size fraction, we repeated the calculations above for in situ production experiments at the two time series stations. On average at the sampling time, the three groups of cells were slightly smaller and/or less numerous throughout the euphotic zone at 0° compared to 3°S. In contrast, mv-chl *a*, dv-chl *a*, and primary production were higher at the equator. Consequently, C:chl *a* ratios were significantly lower and growth rates higher at 0° than at 3°S

**Table 5.** Carbon Content (C, mg $m^{-3}$) of *Prochlorococcus*, *Synechococcus*, and Pico-eukaryotes as Estimated From Flow Cytometry Data[a]

| Latitude | $C_{Proc}$ | $C_{Syn}$ | $C_{Pico}$ | C:chl *a* | $P_C$ | μ |
|---|---|---|---|---|---|---|
| 8°S | 3.1 | 2.7 | 3.5 | 126 | 7.6 | 0.60 |
| 7°S | 7.9 | 2.5 | 3.3 | 118 | 8.8 | 0.50 |
| 5°S | 10.7 | 2.8 | 6.2 | 173 | 11.5 | 0.46 |
| 3°S | 9.7 | 2.5 | 11.8 | 224 | 12.6 | 0.42 |
| 3°S | 13.5 | 3.8 | 12.0 | 169 | 11.3 | 0.33 |
| 2°S | 8.9 | 4.4 | 11.0 | 183 | 15.1 | 0.48 |
| 1°S | 8.5 | 4.2 | 8.2 | 138 | 14.1 | 0.52 |
| 0° | 8.7 | 3.4 | 12.8 | 122 | 21.4 | 0.62 |
| 0° | 11.5 | 4.4 | 11.8 | 133 | 17.5 | 0.49 |
| 1°N | 12.2 | 4.8 | 9.7 | 160 | 19.1 | 0.54 |
| 4°N | 8.6 | 3.3 | 8.0 | 116 | 12.6 | 0.49 |
| 7°N | 1.6 | 0.2 | 1.4 | 70 | 3.7 | 0.77 |

[a]C:chl *a* ratio (g:g), $P_C$ in (mgC $m^{-3}$ $h^{-1}$)12 and growth rate (μ, $d^{-1}$) of phytoplankton in the <3 μm size fraction.

**Table 6.** Carbon Content (Co, mg $m^{-3}$), $P_C$ in (mgC $m^{-3}$ $h^{-1}$)12, Growth Rate ($\mu$, $d^{-1}$) and C:chl *a* Ratio of Phytoplankton in the <3 μm Size Fraction[a]

| Depth | Co | $P_C$ | μ | C:Chla |
|---|---|---|---|---|
| | | *3°S* | | |
| 0 | 27.6 (4.3) | 10.2 (1.0) | 0.32 (0.06) | 220 (12) |
| 5 | 27.8 (4.1) | 10.7 (1.2) | 0.33 (0.07) | 219 (11) |
| 10 | 28.4 (4.0) | 11.0 (0.9) | 0.33 (0.06) | 218 (10) |
| 20 | 27.2 (2.0) | 11.7 (1.1) | 0.36 (0.05) | 193 (7) |
| 30 | 30.3 (1.0) | 11.3 (0.9) | 0.32 (0.03) | 181 (8) |
| 40 | 28.7 (3.4) | 8.8 (2.0) | 0.27 (0.08) | 153 (11) |
| 50 | 24.4 (1.7) | 6.9 (1.4) | 0.25 (0.06) | 132 (12) |
| 60 | 20.4 (1.3) | 4.6 (0.6) | 0.20 (0.02) | 118 (20) |
| 70 | 16.4 (2.2) | 3.7 (0.4) | 0.21 (0.03) | 98 (12) |
| 80 | 12.6 (4.2) | 1.9 (0.3) | 0.15 (0.03) | 80 (17) |
| 100 | 5.8 (1.5) | 0.6 (0.1) | 0.10 (0.03) | 57 (7) |
| | | *0°* | | |
| 0 | 23.0 (2.6) | 12.7 (1.6) | 0.45 (0.02) | 143 (34) |
| 5 | 21.1 (1.8) | 14.3 (1.0) | 0.50 (0.04) | 135 (29) |
| 10 | 20.2 (2.7) | 14.2 (1.6) | 0.53 (0.02) | 128 (24) |
| 20 | 21.5 (4.4) | 13.9 (1.1) | 0.51 (0.10) | 127 (38) |
| 30 | 20.0 (2.8) | 10.8 (1.3) | 0.44 (0.06) | 114 (17) |
| 40 | 19.7 (3.7) | 9.3 (0.1) | 0.39 (0.05) | 106 (21) |
| 50 | 17.7 (2.7) | 6.8 (0.5) | 0.33 (0.04) | 92 (11) |
| 60 | 16.0 (4.2) | 4.3 (0.5) | 0.25 (0.07) | 81 (16) |
| 70 | 15.8 (4.5) | 2.2 (0.8) | 0.14 (0.07) | 78 (17) |
| 80 | 13.6 (2.7) | 1.0 (0.5) | 0.08 (0.05) | 68 (5) |
| 100 | 9.8 (2.2) | 0.3 (0.2) | 0.04 (0.02) | 56 (14) |

[a]Means (±standard deviation) of three profiles at 3°S and 0°.

(Table 6). A similar difference in C:chl *a* was also obtained for *Prochlorococcus* only, on the basis of carbon estimates from flow cytometry and taxon-specific divinyl-chlorophyll *a* (data not shown). As evident also in community-based assessments of C:chl *a* and μ, the <3-μm phytoplankton were richer in chlorophyll and faster growing at the source of the equatorial upwelling than at 3°S. Since PI estimates at these two intensively studied stations were quite comparable (Figure 6), one may conclude that the variations in C:chl *a* and μ were largely offsetting.

[47] Finally, since oligotrophic waters contain relatively more small cells, which potentially grow faster than larger cells under limiting (macronutrient or iron) conditions, one cannot reject the hypothesis that production per unit chlorophyll could be equal, if not higher, at steady state in nitrate-depleted waters compared to the HNLC region. Our observations show that the specific photosynthetic activity of chl *a*, as measured by the $^{14}C$ method under rigorously controlled experimental conditions, appears independent of macronutrient availability in the equatorial Pacific. Furthermore, in situ experiments demonstrate that significant changes in C/chl *a* and μ may occur in the HNLC system without any significant effect on PI. As a consequence, the rate of primary production for a mean sunny day depends mainly on chlorophyll concentration. This property can be applied as a first approximation to predicting primary production from chl *a* data, taking into account the light penetration in the water column. By this simple empirical approach, it is possible to calculate primary production in the equatorial belt of the Pacific Ocean with reasonable accuracy.

### 4.2. Short-Term Variability of Biomass and Production

[48] Pigment variability during 5 d of sampling at two fixed stations indicates that diel fluctuations in chl *a* exert relatively small influences on production estimates compared to geographic variability along the meridian 180°. Assuming that diel changes in chl *a* are always modest along the transect, chlorophyll data collected at any time of the day appear quite suitable for quantifying production by the empirical procedure proposed above. Conversely, in systems where the amplitude of diel variations is larger, as was observed, for example, in the equatorial Atlantic [*Le Bouteiller and Herbland*, 1982], this effect could become significant and should be considered a possible source of error in production appraisals from chl *a* profiles. Nevertheless, the effects of diel changes in chl *a* on production estimates tend to be self-correcting. When chl *a* increases in the euphotic layer during daytime, $Z_{eu}$ shoals and the radiation available at any depth decreases. Consequently, the production enhancement proportional to the chlorophyll increase is smoothed by a relative decrease of PAR. Conversely, in lower chl *a* waters, the reduced production $m^{-3}$ is counterbalanced by a better radiation availability due to a deeper penetration of light, extending euphotic zone.

[49] The remarkably low variance of production values calculated from a reliable and exceptionally intensive chl *a* data set is of significance. It means that the inherent variability of the planktonic system is small despite diel changes and a physically vigorous system. At both the equator and 3°S, the south equatorial current flowed westward with a steady velocity of 0.4–0.6 m $s^{-1}$. Therefore 2 km or more separated hourly hydrocasts, with almost a 45-km separation among water parcels sampled over 24 h. In addition, a rapid twofold decrease of surface nitrate during the second time series station (0°) was ascribed to advection of a different water mass from the east or northeast [*Eldin and Rodier*, 2003]. Even so, despite the >200-km sampling distance separation and the nutrient differences, the depth-integrated production estimates from the first to the fifth day at 0° were quite similar (856 and 833 mgC $m^{-2}$ $d^{-1}$, respectively). These observations suggest that we sampled at each of the two time series stations a similar steady state biological system containing a characteristic assemblage of autotrophic and heterotrophic organisms, almost as if we had followed, in Lagrangian mode, one water mass marked by a perfect drifter. Conversely, for us to have observed repeatedly similar depth distributions of chl *a* and biomass in our Eulerian approach, the same biological system must have been simultaneously present in wide zonal bands parallel to the equator, strongly constrained by the same controlling factors. Therefore the mean production values presented here appear to be representative of a much broader oceanic region than the geographically fixed stations where the samples were collected.

### 4.3. Difference Between 0° and 3°S

[50] Daily fluctuations of phytoplankton biomass around equilibrium levels were significantly higher at 0° than at 3°S, consistent with better growth conditions at the equator as suggested above. By independent assessments for both the total phytoplankton community and the <3-μm size fraction, growth rate was 30–40% higher at the equator than at 3°S. Contemporaneous measurements of the instantaneous rates of phytoplankton growth at the time series stations are consistent with the magnitude of these differences [*Landry et al.*, 2003]. Furthermore, biogenic silica

concentration was also enhanced by >threefold at the equator, $Si(OH)_4$ uptake rate was an order of magnitude greater (2.58 versus 0.33 mmolSi $m^{-2}$ $d^{-1}$), and $NO_3$ uptake and the "f" ratio were higher by factors of 2.6 and 2.5, respectively. These flux differences likely reflect differences in the supply rate of iron, the concentrations and effects of which are unquantified in the current study but well demonstrated in others.

[51] According to *Coale et al.* [1996], the bulk of iron input to equatorial surface waters occurs by advective upwelling from the iron-rich Equatorial Undercurrent rather than atmospheric deposition. Because of the relative proximity of the major source of iron along the northern coast of Papua New Guinea [*Gordon et al.*, 1997; *Mackey et al.*, 2002b], the EUC could be particularly iron-rich at 180° during a cold ENSO episode [*Wells et al.*, 1999]. The upwelling divergence occurs mainly in a 20-km latitude band centered on the equator [*Poulain*, 1993], where the EUC is shallowest (80 m during EBENE). The focused delivery of new iron thus gives the characteristic tongue of enriched chl *a*, which stretches along the equator from the Galapagos Islands to the western upwelling front in CZCS, POLDER and SeaWiFS satellite images under "normal" (i.e., non-El Niño) conditions. During EBENE, equatorial upwelling was active at the 180° meridian, and the HNLC zone extended even further west than typical [*Dupouy et al.*, 2003]. Consequently, the different magnitudes of phytoplankton activity measured at 3°S and 0°, and especially the much higher rates of new production (nitrate and silicate uptake), are consistent with latitudinal difference in iron supply to the upper layer.

[52] Despite differences in "new" nutrient (iron) enrichment, the chl *a* concentrations at 0° were only slightly higher than at 3°S. Clearly, nutrient limitation is not drastic for the small cells *(Prochlorococcus*, *Synechococcus*, and picoeukaryotes) which dominate the phytoplankton communities [*Blanchot et al.*, 2001; *André et al.*, 1999] and compete efficiently for remineralized nitrogen [*Raimbault et al.*, 1999] and iron [*Landry et al.*, 1997]. In fact, the quasi-constant biomass of phytoplankton during intensive sampling of the time series stations reflects a balance between utilization of the limiting resource by phytoplankton and losses to grazing, advection and sedimentation [*Landry et al.*, 1995, 1997; *André et al.*, 1999; *Vaulot and Marie*, 1999; *Le Borgne and Landry*, 2003]. If this ecological equilibrium between phytoplankton requirements and natural resources were qualitatively the same along the transect, then nutrient stress would be of a similar intensity everywhere, implying a great monotony of photosynthetic efficiency and growth rate. By itself, the uniform distribution of PI reported here would tend to support such a view. However, other field measurements demonstrate a more complicated reality. Observations at 3°S and 0° exhibited substantial differences in rates of growth and new production. Such differences could not have been suspected from a simple examination of macronutrient or chl *a* concentrations.

[53] **Acknowledgments.** We would like to thank the crew of the R/V *L'Atalante* for their assistance, especially during operations of launching and recovery of in situ production arrays. We thank Nicole Garcia for $^{15}N$ analyses by mass spectrometry in Marseille. Financial support for this work was provided by IRD and INSU-CNRS.

## References

André, J.-M., C. Navarette, J. Blanchot, and M.-H. Radenac, Picophytoplankton dynamics in the equatorial Pacific: Growth and grazing rates from cytometric counts, *J. Geophys. Res.*, *104*, 3368–3380, 1999.

Archer, D., et al., A meeting place of great ocean currents: Shipboard observations of a convergent front at 2°N in the Pacific, *Deep Sea Res., Part II*, *44*, 1827–1849, 1997.

Aufdenkampe, A. K., J. J. McCarthy, C. Navarette, M. Rodier, J. Dunne, and J. W. Murray, Biogeochemical controls on new production in the tropical Pacific, *Deep Sea Res., Part II*, *49*, 2619–2648, 2002.

Banse, K., Grazing and zooplankton production as key controls of phytoplankton production in the open ocean, *Oceanography*, *7*, 13–20, 1994.

Banse, K., Zooplankton: Pivotal role in the control of ocean production, *ICES J. Mar. Sci.*, *52*, 265–277, 1995.

Barber, R. T., M. P. Sanderson, S. T. Lindley, F. Chai, J. Newton, C. C. Trees, D. G. Foley, and F. P. Chavez, Primary productivity and its regulation in the equatorial Pacific during and following the 1991–1992 El Niño, *Deep Sea Res., Part II*, *43*, 933–969, 1996.

Blanchot, J., J.-M. André, C. Navarette, J. Neveux, and M.-H. Radenac, Picophytoplankton in the equatorial Pacific: Vertical distributions in the warm pool and in the high nutrient low chlorophyll conditions, *Deep Sea Res., Part A*, *48*, 297–314, 2001.

Brown, S. L., M. R. Landry, J. Neveux, and C. Dupouy, Microbial community abundance and biomass along a 180° transect in the equatorial Pacific during an El Niño-Southern Oscillation cold phase, *J. Geophys. Res.*, *108*(C12), 8139, doi:10.1029/2001JC000817, in press, 2003.

Brzezinski, M. A., The Si:C:N ratio of marine diatoms: Interspecific variability and the effect of some environmental variables, *J. Phycol.*, *21*, 347–357, 1985.

Buesseler, K. O., Understanding the coupling between primary production and particulate export in the upper ocean, *Eos Trans. AGU*, *79*(1), Ocean Sci. Meet. Suppl., 0595, 1998.

Cavender-Bares, K. K., E. L. Mann, S. W. Chisholm, M. E. Ondrusek, and R. R. Bidigare, Differential response of equatorial Pacific phytoplankton to iron fertilization, *Limnol. Oceanogr.*, *44*, 455–466, 1999.

Chavez, F. P., Size distribution of phytoplankton in the central and eastern tropical Pacific, *Global Biogeochem. Cycles*, *3*, 27–35, 1989.

Chavez, F. P., and J. R. Toggweiler, Physical estimates of global new production: The upwelling contribution, in *Upwelling in the Ocean: Modern Processes and Ancient Records*, edited by C. P. Summerhayes et al., pp. 313–320, John Wiley, Hoboken, N. J., 1995.

Chavez, F. P., K. R. Buck, K. H. Coale, J. H. Martin, G. R. DiTullio, N. A. Welschmeyer, A. C. Jacobson, and R. T. Barber, Growth rates, grazing, sinking, and iron limitation of equatorial Pacific phytoplankton, *Limnol. Oceanogr.*, *36*, 1816–1833, 1991.

Chavez, F. P., K. R. Buck, S. K. Service, J. Newton, and R. T. Barber, Phytoplankton variability in the central and eastern tropical Pacific, *Deep Sea Res., Part II*, *43*, 835–870, 1996.

Chavez, F. P., P. G. Strutton, G. E. Friederich, R. A. Feely, G. C. Feldman, D. G. Foley, and M. J. McPhaden, Biological and chemical response of the equatorial Pacific Ocean to the 1997–98 El Niño, *Science*, *286*, 2126–2131, 1999.

Claustre, H., A. Morel, M. Babin, C. Cailliau, D. Marie, J.-C. Marty, D. Tailliez, and D. Vaulot, Variability in particle attenuation and chlorophyll fluorescence in the tropical Pacific: Scales, patterns, and biogeochemical implications, *J. Geophys. Res.*, *104*, 3401–3422, 1999.

Coale, K. H., S. E. Fitzwater, R. M. Gordon, K. S. Johnson, and R. T. Barber, Control of community growth and export production by upwelled iron in the equatorial Pacific Ocean, *Nature*, *379*, 621–624, 1996.

Cullen, J. J., M. R. Lewis, C. O. Davis, and R. T. Barber, Photosynthetic characteristics and estimated growth rates indicate grazing is the proximate control of primary production in the equatorial Pacific, *J. Geophys. Res.*, *97*, 639–654, 1992.

Curl, H., Jr., and L. F. Small, Variations in photosynthetic assimilation ratios in natural, marine phytoplankton communities, *Limnol. Oceanogr.*, *10*, R67–R73, 1965.

Dortch, Q., The interaction between ammonium and nitrate uptake in phytoplankton, *Mar. Ecol. Prog. Ser.*, *61*, 183–201, 1990.

Dugdale, R. C., and F. P. Wilkerson, The use of $^{15}N$ to measure nitrogen uptake in eutrophic oceans: Experimental conditions, *Limnol. Oceanogr.*, *31*, 673–689, 1986.

Dugdale, R. C., and F. P. Wilkerson, Low specific nitrate uptake rate: A common feature of high-nutrient, low-chlorophyll marine ecosystems, *Limnol. Oceanogr.*, *36*, 1678–1688, 1991.

Dugdale, R. C., F. P. Wilkerson, R. T. Barber, and F. P. Chavez, Estimating new production in the equatorial Pacific Ocean at 150°W, *J. Geophys. Res.*, *97*, 681–686, 1992.

Dupouy, C., H. Oiry, A. Le Bouteiller, and M. Rodier, Variability of the equatorial phytoplankton enrichment in the western Pacific Ocean, in

*Satellite Remote Sensing of the Ocean*, edited by I. S. F. Jones et al., pp. 406–418, Seibutsu Kenkyusha, Tokyo, 1993.

Dupouy, C., H. Loisel, J. Neveux, S. L. Brown, C. Moulin, J. Blanchot, A. Le Bouteiller, and M. R. Landry, Microbial absorption and backscattering coefficients from in situ and POLDER satellite data during an El Niño-Southern Oscillation cold phase in the equatorial Pacific (180°), *J. Geophys. Res.*, *108*(C12), 8138, doi:10.1029/2001JC001298, in press, 2003.

Eldin, G., and M. Rodier, Ocean physics and nutrient fields along 180 during an El Niño-Southern Oscillation cold phase, *J. Geophys. Res.*, *108*(C12), 8137, doi:10.1029/2000JC000746, in press, 2003.

Eppley, R. W., and B. J. Peterson, Particulate organic matter flux and planktonic new production in the deep ocean, *Nature*, *282*, 677–680, 1979.

Eppley, R. W., F. M. H. Reid, and J. D. H. Strickland, Estimates of phytoplankton crop size, growth rate, and primary production, in *The Ecology of the Plankton off La Jolla, California, in the Period APRIL through September*, *1967*, edited by J. D. H. Strickland, *Bull. Sripps Inst. Oceanogr.*, *17*, 33–42, 1970.

Fitzwater, S. E., G. A. Knauer, and J. H. Martin, Metal contamination and its effect on primary production measurements, *Limnol. Oceanogr.*, *27*, 544–551, 1982.

Frost, B. W., and N. C. Franzen, Grazing and iron limitation in the control of phytoplankton stock and nutrient concentration: A chemostat analogue of the Pacific equatorial upwelling zone, *Mar. Ecol. Prog. Ser.*, *83*, 291–303, 1992.

Gaudy, R., G. Champalbert, and R. Le Borgne, Feeding and metabolism of mesozooplankton in the equatorial Pacific high-nutrient, low-chlorophyll zone along 180°, *J. Geophys. Res.*, *108*(C12), 8144, doi:10.1029/2000JC000743, in press, 2003.

Goldman, J. C., and M. R. Dennett, Susceptibility of some marine phytoplankton species to cell breakage during filtration and post-filtration, *J. Exp. Mar. Biol. Ecol.*, *86*, 47–58, 1985.

Gordon, R. M., K. H. Coale, and K. S. Johnson, Iron distributions in the equatorial Pacific: Implications for new production, *Limnol. Oceanogr.*, *42*, 419–431, 1997.

Guérédrat, J. A., Evolution d'une population de copépodes dans le système des courants équatoriaux de l'Océan Pacifique: Zoogéographie, écologie et diversité spécifique, *Mar. Biol.*, *9*, 300–314, 1971.

Herbland, A., and A. Le Bouteiller, Dynamique du phytoplancton et matière organique particulaire dans la zone euphotique de l'Atlantique Equatorial, *Mar. Biol.*, *72*, 265–278, 1983.

Holm-Hansen, O., and B. Riemann, Chlorophyll *a* determination: Improvements in methodology, *Oikos*, *30*, 438–447, 1978.

Karl, D. M., D. V. Hebel, and R. M. Letelier, The role of dissolved organic matter release in the productivity of the oligotrophic North Pacific Ocean, *Limnol. Oceanogr.*, *43*, 1270–1286, 1998.

Kemp, A. E. S., R. B. Pearce, I. Koizumi, J. Pike, and S. J. Rance, The role of mat-forming diatoms in the formation of Mediterranean sapropels, *Nature*, *398*, 57–61, 1999.

Landry, M. R., J. Constantinou, and J. D. Kirshtein, Microzooplankton grazing in the central equatorial Pacific during February and August, 1992, *Deep Sea Res., Part II*, *42*, 657–671, 1995.

Landry, M. R., et al., Iron and grazing constraints on primary production in the central Pacific: An EqPac synthesis, *Limnol. Oceanogr.*, *42*, 405–418, 1997.

Landry, M. R., M. E. Ondrusek, S. J. Tanner, S. L. Brown, J. Constantinou, R. R. Bidigare, K. H. Coale, and S. Fitzwater, Biological response to iron fertilization in the eastern equatorial Pacific (IronEx II). I. Microplankton community abundances and biomass, *Mar. Ecol. Prog. Ser.*, *201*, 27–42, 2000a.

Landry, M. R., J. Constantinou, M. Latasa, S. L. Brown, R. R. Bidigare, and M. E. Ondrusek, Biological response to iron fertilization in the eastern equatorial Pacific (IronEx II). III. Dynamics of phytoplankton growth and microzooplankton grazing, *Mar. Ecol. Prog. Ser.*, *201*, 57–72, 2000b.

Landry, M. R., S. L. Brown, J. Neveux, C. Dupouy, J. Blanchot, S. Christensen, and R. R. Bidigare, Phytoplankton growth and microzooplankton grazing in high-nutrient, low-chlorophyll waters of the equatorial Pacific: Community and taxon-specific rate assessments from pigment and flow cytometric analyses, *J. Geophys. Res.*, *108*(C12), 8142, doi:10.1029/2000JC000744, in press, 2003.

Laws, E. A., and D. C. Wong, Studies of carbon and nitrogen metabolism by three marine phytoplankton species in nitrate-limited continuous culture, *J. Phycol.*, *14*, 406–416, 1978.

Laws, E. A., D. G. Redalje, L. W. Haas, P. K. Bienfang, R. W. Eppley, W. G. Harrison, D. M. Karl, and J. Marra, High phytoplankton growth and production rates in oligotrophic Hawaiian coastal waters, *Limnol. Oceanogr.*, *29*, 1161–1169, 1984.

Laws, E. A., G. R. DiTullio, and D. G. Redalje, High phytoplankton growth and production rates in the North Pacific subtropical gyre, *Limnol. Oceanogr.*, *32*, 905–918, 1987.

Laws, E. A., G. R. DiTullio, P. R. Betzer, D. M. Karl, and K. L. Carder, Autotrophic production fluxes at 26°N, 155°W in the North Pacific subtropical gyre, *Deep Sea Res., Part A*, *36*, 103–120, 1989.

Laws, E. A., G. R. DiTullio, K. L. Carder, P. R. Betzer, and S. Hawes, Primary production in the deep blue sea, *Deep Sea Res., Part A*, *37*, 715–730, 1990.

Le Borgne, R., and M. R. Landry, EBENE: A JGOFS investigation of plankton variability and trophic interactions in the equatorial Pacific (180°), *J. Geophys. Res.*, *108*(C12), 8136, doi:10.1029/2001JC001252, in press, 2003.

Le Borgne, R., M. Rodier, A. Le Bouteiller, and J. W. Murray, Zonal variability of plankton and particle flux in the equatorial Pacific upwelling between 165°E and 150°W, *Oceanol. Acta*, *22*, 57–66, 1999.

Le Bouteiller, A., and J. Blanchot, Size distribution and abundance of phytoplankton in the Pacific equatorial upwelling, *Mer*, *29*, 175–179, 1991.

Le Bouteiller, A., and A. Herbland, Diel variation of chlorophyll a as evidenced from a 13 day station in the equatorial Atlantic Ocean, *Oceanol. Acta*, *5*, 433–441, 1982.

Le Bouteiller, A., and A. Herbland, Carbon fixation and productivity index in relation to chlorophyll and light in the equatorial Atlantic Ocean, *Oceanogr. Trop.*, *19*, 161–179, 1984.

Le Bouteiller, A., J. Blanchot, and M. Rodier, Size distribution patterns of phytoplankton in the western Pacific: Towards a generalization for the tropical open ocean, *Deep Sea Res., Part A*, *39*, 805–823, 1992.

Legendre, L., and J. Le Fèvre, Hydrodynamic singularities as controls of recycled versus export production in oceans, in *Productivity of the Ocean: Present and Past*, edited by W. H. Berger et al., pp. 49–63, John Wiley, Hoboken, N. J., 1989.

Leynaert, A., P. Tréguer, C. Lancelot, and M. Rodier, Silicon limitation of biogenic silica production in the equatorial Pacific, *Deep Sea Res., Part A*, *48*, 639–660, 2001.

Lindley, S. T., R. R. Bidigare, and R. T. Barber, Phytoplankton photosynthesis parameters along 140°W in the equatorial Pacific, *Deep Sea Res., Part II*, *42*, 441–463, 1995.

Liu, H. L., M. R. Landry, D. Vaulot, and L. Campbell, Prochlorococcus growth rates in the central equatorial Pacific: An application of the $f_{max}$ approach, *J. Geophys. Res.*, *104*, 3391–3399, 1999.

Mackey, D. J., J. Blanchot, H. W. Higgins, and J. Neveux, Phytoplankton abundances and community structure in the equatorial Pacific, *Deep Sea Res., Part II*, *49*, 2561–2582, 2002a.

Mackey, D. J., J. E. O'Sullivan, and R. J. Watson, Iron in the western Pacific: A riverine or hydrothermal source for iron in the Equatorial Undercurrent?, *Deep Sea Res., Part I*, *49*, 877–893, 2002b.

Mann, E. L., and S. W. Chisholm, Iron limits the cell division rate of *Prochlorococcus* in the eastern equatorial Pacific, *Limnol. Oceanogr.*, *45*, 1067–1076, 2000.

Martin, J. H., R. M. Gordon, and S. E. Fitzwater, The case for iron, *Limnol. Oceanogr.*, *36*, 1793–1802, 1991.

McCarthy, J. J., C. Garside, and J. L. Nevins, Nitrate supply and phytoplankton uptake kinetics in the euphotic layer of a Gulf Stream warm-core ring, *Deep Sea Res., Part A*, *39*, suppl. 1, S393–S403, 1992.

McCarthy, J. J., C. Garside, J. L. Nevins, and R. T. Barber, New production along 140°W in the equatorial Pacific during and following the 1992 El Niño event, *Deep Sea Res., Part II*, *43*, 1065–1093, 1996.

Minas, H. J., M. Minas, and T. T. Packard, Productivity in upwelling areas deduced from hydrographic and chemical fields, *Limnol. Oceanogr.*, *31*, 1182–1206, 1986.

Morel, A., Optical modeling of the upper ocean in relation to its biogenous matter content (case I waters), *J. Geophys. Res.*, *93*, 10,749–10,768, 1988.

Morel, F. M. M., R. J. M. Hudson, and N. M. Price, Limitation of productivity by trace metals in the sea, *Limnol. Oceanogr.*, *36*, 1742–1755, 1991.

Murray, J. W., R. T. Barber, M. R. Roman, M. P. Bacon, and R. A. Feely, Physical and biological controls on carbon cycling in the equatorial Pacific, *Science*, *266*, 58–65, 1994.

Navarette, C., Dynamique du phytoplancton en océan équatorial: Mesures cytométriques et mesures isotopiques durant la campagne FLUPAC en Octobre 1994 dans la partie ouest du Pacifique, Ph.D. thesis, pp. 313, Univ. Paris, Paris, 1998.

Neveux, J., C. Dupouy, J. Blanchot, A. Le Bouteiller, M. R. Landry, and S. L. Brown, Diel dynamics of chlorophylls in high-nutrient, low-chlorophyll waters of the equatorial Pacific (180°): Interactions of growth, grazing, physiological responses, and mixing, *J. Geophys. Res.*, *108*(C12), 8140, doi:10.1029/2000JC000747, in press, 2003.

Peña, M. A., M. R. Lewis, and W. G. Harrison, Primary productivity and size structure of phytoplankton biomass on a transect of the equator at 135°W in the Pacific Ocean, *Deep Sea Res., Part A*, *37*, 295–315, 1990.

Peña, M. A., W. G. Harrison, and M. R. Lewis, New production in the central equatorial Pacific, *Mar. Ecol. Prog. Ser.*, *80*, 265–274, 1992.

Platt, T., S. Sathyendranath, O. Ulloa, W. G. Harrison, N. Hoepffner, and J. Goes, Nutrient control of phytoplankton photosynthesis in the western North Atlantic, *Nature*, *356*, 229–231, 1992.

Poulain, P.-M., Estimates of horizontal divergence and vertical velocity in the equatorial Pacific, *J. Phys. Oceanogr.*, *23*, 601–607, 1993.

Price, N. M., B. A. Ahner, and F. M. M. Morel, The equatorial Pacific Ocean: Grazer-controlled phytoplankton populations in an iron-limited ecosystem, *Limnol. Oceanogr.*, *39*, 520–534, 1994.

Ragueneau, O., et al., A review of the Si cycle in the modern ocean: Recent progress and missing gaps in the application of biogenic opal as a paleoproductivity proxy, *Global Planet. Change*, *26*, 317–365, 2000.

Raimbault, P., G. Slawyk, B. Boudjellal, C. Coatanoan, P. Conan, B. Coste, N. Garcia, T. Moutin, and M. Pujo-Pay, Carbon and nitrogen uptake and export in the equatorial Pacific at 150°W: Evidence of an efficient regenerated production cycle, *J. Geophys. Res.*, *104*, 3341–3356, 1999.

Raimbault, P., G. Slawyk, and N. Garcia, Comparison between chemical and isotopic measurements of biological nitrate utilization: Further evidence of low new production levels in the equatorial Pacific, *Mar. Biol.*, *136*, 1147–1155, 2000.

Reverdin, G., A. Morlière, and G. Eldin, ALIZE 2, Campagne océanographique trans-Pacifique, report, 341 pp., Lab. d'Oceanogr. Dyn. et de Climatol., Univ. Pierre et Marie Curie, Paris, 1991.

Rodier, M., and R. Le Borgne, Export flux of particules at the equator in the western and central Pacific Ocean, *Deep Sea Res., Part II*, *44*, 2085–2113, 1997.

Snedecor, G. W., and W. G. Cochran, *Statistical Methods*, 6th ed., 593 pp., Iowa State Univ. Press, Ames, 1967.

Strathmann, R. S., Estimating the organic carbon content of phytoplankton from cell volume or plasma volume, *Limnol. Oceanogr.*, *12*, 411–418, 1967.

Strutton, P. G., and F. P. Chavez, Primary productivity in the equatorial Pacific during the 1997–1998 El Niño, *J. Geophys. Res.*, *105*, 26,089–26,101, 2000.

Sunda, W. G., and S. A. Huntsman, Interrelated influence of iron, light and cell size on marine phytoplankton growth, *Nature*, *390*, 389–392, 1997.

Tans, P. P., I. Y. Fung, and T. Takahashi, Observational constraints on the global atmospheric $CO_2$ budget, *Science*, *247*, 1431–1438, 1990.

Thingstad, T. F., A theoretical approach to structuring mechanisms in the pelagic food web, *Hydrobiology*, *363*, 59–72, 1998.

Thomas, W. H., On the nitrogen deficiency in tropical Pacific oceanic phytoplankton: Photosynthetic parameters in poor and rich water, *Limnol. Oceanogr.*, *15*, 380–385, 1970.

Vaulot, D., and D. Marie, Diel variability of photosynthetic picoplankton in the equatorial Pacific, *J. Geophys. Res.*, *104*, 3297–3310, 1999.

Verity, P. G., C. Y. Robertson, C. R. Tronzo, M. G. Andrews, J. R. Nelson, and M. E. Sieracki, Relationships between cell volume and the carbon and nitrogen content of marine photosynthetic nanoplankton, *Limnol. Oceanogr.*, *37*, 1434–1446, 1992.

Walsh, J. J., Herbivory as a factor in patterns of nutrient utilization in the sea, *Limnol. Oceanogr.*, *21*, 1–13, 1976.

Wells, M. L., G. K. Vallis, and E. A. Silver, Tectonic processes in Papua New Guinea and past productivity in the eastern equatorial Pacific Ocean, *Nature*, *398*, 601–604, 1999.

Wheeler, P. A., and S. A. Kokkinakis, Ammonium recycling limits nitrate use in the oceanic subarctic Pacific, *Limnol. Oceanogr.*, *35*, 1267–1278, 1990.

Wyrtki, K., Sea level and seasonal fluctuations of the equatorial currents in the western Pacific Ocean, *J. Phys. Oceanogr.*, *4*, 91–103, 1974.

Wyrtki, K., An estimate of equatorial upwelling in the Pacific, *J. Phys. Oceanogr.*, *11*, 1205–1214, 1981.

J. Blanchot, Institut de Recherche pour le Développement (IRD)-Sainte Clotilde, St. Clotilde, 97940 La Réunion, France.

S. L. Brown and M. R. Landry, Department of Oceanography, University of Hawaii at Manoa, 1000 Pope Rd., Honolulu, HI 96822, USA.

R. Le Borgne, A. Le Bouteiller, and M. Rodier, Institut de Recherche pour le Développement, BP A5, 98 848 Nouméa, Nouvelle-Calédonie, France. (leboutei@noumea.ird.nc)

A. Leynaert, Institut Universitaire Européen de la Mer, 29280 Plouzané, France.

J. Neveux, Observatoire Océanologique de Banyuls (CNRS-UPMC), Laboratoire Arago (UMR 7621), BP44, 66651 Banyuls sur Mer, France.